

The inhomogeneous Fermi-Pasta-Ulam chain, a case study of the 1 : 2 : 3 resonance

Roelof Bruggeman and Ferdinand Verhulst
Mathematisch Instituut, PO Box 80.010
3508TA Utrecht, Netherlands

March 20, 2018

Running title: The inhomogeneous Fermi-Pasta-Ulam chain
MSC classification: 70H07, 70H12, 34E10, 37J40

Abstract

The inhomogeneous Fermi-Pasta-Ulam chain is studied by identifying the mass ratios that produce prominent resonances. This is a technically complicated problem as we have to solve an inverse problem for the spectrum of the corresponding linearized equations of motion. In the case of the inhomogeneous periodic Fermi-Pasta-Ulam chain with four particles each mass ratio determines a frequency ratio for the quadratic part of the Hamiltonian. Most prominent frequency ratios occur but not all. In general we find a one-dimensional variety of mass ratios for a given frequency ratio.

For the resonance 1 : 2 : 3 a small cubic term added to the Hamiltonian leads to a dynamical behaviour that shows a difference between the case that two masses are equal and the more general case of four different masses. For two equal masses the normalized system is integrable and chaotic behaviour is small-scale. In the transition to four different masses we find a Hamiltonian-Hopf bifurcation of one of the normal modes leading to complex instability and Shilnikov-Devaney bifurcation. The other families of short-periodic solutions can be localized from the normal forms together with their stability characteristics. For illustration we use action simplices and the behaviour with time of the H_2 integral of the normal forms.

1 Introduction

The Fermi-Pasta-Ulam (FPU) chain or lattice is an n degrees-of-freedom (dof) Hamiltonian system that models a chain of oscillators with nearest-neighbour interaction, see [5] and [6]. We will describe the model in section 2, see also [9]. There exists a huge amount of literature on the FPU chain but nearly always regarding the case of equal masses, sometimes called the mono-atomic case. In this paper we will outline a research program to study the inhomogeneous case where the masses are different. An inhomogeneous nonlinear lattice with nearest neighbour interaction is studied in [14] with emphasis on energy control. It is understandable that only a few results were obtained for inhomogeneous lattices as the choice of inhomogeneities, the masses of the lattice, seems to be arbitrary. We will solve this arbitrariness by focusing on the presence of resonances induced by the choice of masses. After

referring to some basic material on Hamiltonians and normal forms we formulate in section 2 the periodic FPU α chain with arbitrary (positive) masses. In such a n degrees-of-freedom system there exists a momentum integral that enables us to reduce to a $n - 1$ dof system. An inverse problem is considered in section 3: how do we find mass distributions producing prominent resonances in the spectrum induced by $H_2(p, q)$? This involves the analysis of the inverse map of the vector of mass distribution to the vector of positive eigenvalues of an associated coefficient matrix. This problem is solved in section 3 for the cases of 3 and 4 particles; in the latter case it turns out that of the four 1st order resonances that exist in general (see for the terminology [13]) 3 exist, of the 12 possible 2nd order resonances 10 exist in this FPU problem. In section 4 we focus on the 1 : 2 : 3 resonance that arises for a one-dimensional variety of mass ratios. It turns out that for one particular combination of mass ratios, the normal form of the nonlinear system is integrable. Moving from this particular case into the variety of mass ratios, one of the periodic solutions shows Hamilton-Hopf bifurcation that corresponds with Shilnikov-Devaney bifurcation in this Hamiltonian system and produces a chaotic normal form.

The appendix contains general statements on the relation between mass ratios and the spectrum induced by $H_2(p, q)$ that can be useful for future research. Table 3 summarises the instructions for the case of 4 particles. It is shown that for a given n -dimensional eigenvector characterizing the FPU chain, all positive solutions of an n -dimensional mass distribution are in a compact subset of \mathbb{R}^n . This subset is empty in some cases, for instance the important 1 : 1 : ... : 1 resonance does not arise for the periodic FPU α chain with four or more particles.

1.1 Hamiltonian formulation

For an autonomous Hamiltonian system with n degrees-of-freedom (dof), n independent integrals suffice for integrability, in that case there will be no chaotic motion in such a system. However, in general, Hamiltonian systems with two or more degrees-of-freedom (dof) are non-integrable. In many cases, this phenomenon was identified with homoclinic chaos as predicted by Poincaré in the nineteenth century, see [10], vol. 3; for a description see [17], sections 5.4 and 9.3.

In the seventies of last century, a number of scientists started with the computation and analysis of normal forms of general Hamiltonian systems near equilibrium. Introductions and surveys of results can be found in [13], chapter 10 and [18]. One starts with an n degrees-of-freedom system with Hamiltonian $H(p, q)$ that can be expanded near equilibrium to a certain order as:

$$H(p, q) = H_2(p, q) + H_3(p, q) + \dots + H_m(p, q) + \dots$$

The index m indicates the degree in the variables (p, q) of the homogeneous polynomial H_m . Sometimes, other coordinate systems are useful, for instance action-angle variables $\tau_i, \phi_i, i = 1 \dots n$. The normal form technique was developed by Poincaré, Birkhoff and modern scientists using analytic and algebraic tools. A basic element is that the resonances that exist near equilibrium produce resonant terms that are kept in the normal form while the non-resonant terms are averaged away. Such a normal form $\bar{H}(p, q)$ does generally not converge when $m \rightarrow \infty$, but a finite expansion contains already a lot of quantitative and qualitative information. The respective polynomials $H_m(p, q), m = 3, 4, \dots$ are after normalization indicated by $\bar{H}_m(p, q)$.

Usually, consideration of a neighbourhood of stable equilibrium is made explicit by scaling with a small positive parameter ε $p \rightarrow \varepsilon p$, $q \rightarrow \varepsilon q$ and dividing the resulting Hamiltonian by ε^2 . The terms H_m , $m \geq 2$ have the coefficient ε^{m-2} . As the normalization is canonical,

$$\bar{H}(p, q) = H_2(p, q) + \varepsilon \bar{H}_3(p, q) + \dots + \varepsilon^{m-2} \bar{H}_m(p, q)$$

is the Hamiltonian integral of the normal form to degree m , whereas, because of the normal form technique, also $H_2(p, q)$ is an integral of the normal form system. This means that two degrees-of-freedom Hamiltonian normal forms are always integrable, they contain no chaos.

1. Hamiltonian normal forms of three or more dof are generally non-integrable; for a recent survey see [18]. In the present paper we will explore to some extent the presence of first and second order resonances for the inhomogeneous FPU problem. The results for the occurrence of resonances will be summarized in table 1.
2. The presence of prominent (first and second order) resonances suggests a research programme outlined in subsection 1.3. For illustration and as a start we will study the $1 : 2 : 3$ resonance for the inhomogeneous FPU problem in the case of four oscillators in a so-called periodic α -chain.

It is standard to use action-angle variables $\tau_i, \phi_i, i = 1, \dots, n$ near stable equilibrium:

$$p_i = \sqrt{2\tau_i} \cos \phi_i, \quad q_i = \sqrt{2\tau_i} \sin \phi_i, \quad i = 1, 2, \dots, n. \quad (1)$$

The equations of motion in action-angle variables are after transforming $p, q \rightarrow \tau, \phi$:

$$\dot{\tau}_i = -\frac{\partial H}{\partial \phi_i}, \quad \dot{\phi}_i = \frac{\partial H}{\partial \tau_i}, \quad i = 1, 2, \dots, n; \quad n \geq 3$$

However, using action-angle variables, special care is needed near the normal modes. After giving arguments in the next subsection, we will use co-moving coordinates in the coordinate planes or whenever an action is near zero. Also, we will often use polar coordinates instead of action-angle variables for orbits in general position; although such transformations are not canonical, they preserve the energy, are easier to establish the effect of resonances and most importantly, they produce qualitatively and quantitatively mathematically equivalent results to action-angle variables (for estimates see [13]).

In the sequel, a periodic solution should be understood as a periodic solution for a fixed value of the energy (iso-energetic solution), so actually it corresponds for the full Hamiltonian system with a family of periodic solutions parameterized by the energy.

1.2 On normal forms and Floquet exponents

Normal form computations for Hamiltonian systems can be carried out in various ways. Apart from efficiency, the main point is to keep the system energy-preserving and preferably canonical. Using for instance action-angle coordinates (1) or amplitude-phase coordinates one can perform averaging over the angles or explicitly time to obtain a first-order normal form. One may consult [13] for more details. An introductory text is [15], chapters 11 and 12.

In section 4 we will analyze periodic α -chains (FPU chains where the Hamiltonian is truncated after the cubic terms), containing the $1 : 2 : 3$ resonance with main objective

to investigate the stability of the short-periodic solutions on the energy manifold and the integrability of the normal form. This is highly relevant for the characterization of the chaotic dynamics of the system but, as mentioned above, it raises special problems. In the cases of vanishing actions or amplitudes, for instance when studying normal modes, the procedure will be as follows (see also section 4.1).

Starting with the equations of motion, we will use co-moving coordinates (see for instance transformation (11.9-10) in chapter 11 of [15]) to obtain a first order normal form. This normal form is used to localize the short-periodic solutions; the normal form conserves the energy but the transformation is not canonical. We will use averaging-normalization as it yields rigorous approximation results (see [13]), the results are qualitatively and quantitatively precise. The same holds when we use polar coordinates outside the coordinate planes. In section 4, the short-periodic solutions can be computed explicitly. The next step is then to linearize near the periodic solutions and to determine the Floquet exponents for which we have to study coupled Mathieu equations. This is still a formidable task, but we can obtain a first order approximation of the exponents by normalizing the coupled Mathieu equations. This will give a number of stability results in section 4.

1.3 Outline of a research programme

The original Fermi-Pasta-Ulam chain [5] consists of n oscillators of equal mass with nearest-neighbour interaction; the chain will be described in the next section. Thousands of papers and a number of conferences were devoted to FPU chains, its stimulus for nonlinear science has been enormous. Among the various problem formulations there was one (nearly always) constant element: the masses of the chain were taken equal. We will present here arguments for considering other mass distributions.

In a neighbourhood of equilibrium, the spectrum of the linear part of the equations of motion plays a crucial part regarding the nature of the ensuing dynamics, see for instance [13] or [18]. Considering inhomogeneous mass distributions in FPU chains, one can produce a great many different spectra induced by H_2 . Each of these cases may produce different dynamics in the corresponding FPU chain. In section 3 we will consider resonant spectra for the case of three and more extensively four particles with periodic boundary conditions i.e. chains where the first and the last oscillator are identified. For the case of four particles we will focus on the rich dynamics of the $1 : 2 : 3$ resonance. An outline of possible further research follows here:

1. According to table 1 regarding the case of four particles, we also have to study two first order resonances ($1 : 2 : 1$ and $1 : 2 : 4$) and ten second order resonances. Also, higher order resonances may be worthwhile to investigate. Special attention should be given to the $1 : 1 : 2$ and $1 : 1 : 3$ cases as only four special mass ratios produce these resonances. In such a case degenerations may arise so that we have to consider detuning phenomena, see [13].
2. Cases of five and more particles will present many more problems.
3. The present study is restricted to so-called periodic α -chains. Including quartic terms in the Hamiltonian (β -chains) and considering lattices with fixed begin- and end-point will produce new results.

4. The study presented here and possibly future studies will throw light on qualitative and quantitative differences between systems in nearest-neighbour interaction and non-local interaction, a topic that is relevant for plasma physics and stellar dynamics.

2 The Fermi-Pasta-Ulam chain

The FPU-chain with periodic boundary conditions has been a topic for many studies. It describes a model for nonlinear interaction of identical point masses moving on a circle with nearest-neighbour coupling. Numerical integrations in the early 1950s showed that the expectation by physicists of thermalisation by energy transport was not correct. Putting all the energy originally in one mode, it was observed that this energy was shared by only a few other modes. Nice introductions can be found in [6] and [9].

For the mono-atomic case of the original periodic FPU-problem (all masses equal) it was shown in [11] for up to six degrees-of-freedom (dof) and much more general in [12], that the corresponding normal forms are governed by 1 : 1 resonances and that these Hamiltonian normal forms are integrable. This explains the recurrence phenomena near equilibrium.

We will drop the original assumption of identical (mono-atomic) particles to consider the periodic FPU-problem again. For n particles with mass $m_j > 0$, position q_j and momentum $p_j = m_j \dot{q}_j$, $j = 1 \dots n$, $\varepsilon \geq 0$ a small parameter, the Hamiltonian is of the form:

$$H(p, q) = \sum_{j=1}^n \left(\frac{1}{2m_j} p_j^2 + V(q_{j+1} - q_j) \right) \text{ with } V(z) = \frac{1}{2}z^2 + \varepsilon \frac{\alpha}{3} z^3 + \varepsilon^2 \frac{\beta}{4} z^4. \quad (2)$$

The quadratic part of the Hamiltonian is not in diagonal form; for $n = 3, 4 \dots$ the linearized equations of motion can be written as:

$$\begin{cases} m_1 \ddot{q}_1 + 2q_1 - q_2 - q_n & = 0, \\ m_2 \ddot{q}_2 + 2q_2 - q_3 - q_1 & = 0, \\ m_3 \ddot{q}_3 + 2q_3 - q_4 - q_2 & = 0, \\ \dots & \dots \\ m_n \ddot{q}_n + 2q_n - q_1 - q_{n-1} & = 0. \end{cases} \quad (3)$$

We can write for the quadratic part of $H(p, q)$:

$$H_2 = \frac{1}{2} p^T A_n p + \frac{1}{2} q^T C_n q, \quad (4)$$

with A_n the $n \times n$ diagonal matrix with at position (i, i) the value $m_i^{-1} =: a_i$, C_n is an $n \times n$ matrix. For an analysis of the quadratic term $H_2(p, q)$ we need to know the eigenvalues of $A_n C_n$. The relation between the eigenvalues of $A_n C_n$ and the eigenvalues of the matrix of coefficients of system (3) will be given below. Since the null space of C_n has dimension one, the matrix $A_n C_n$ has an eigenvalue 0 corresponding to a (translational) momentum integral. It will turn out that the other eigenvalues of $A_n C_n$ are positive, as expected. For a given set of masses, the calculation of the remaining eigenvalues corresponding with the frequencies of the linearized system is easy, but we are faced with another, an inverse problem. To focus ideas, suppose that $n = 4$. The presence of the momentum integral implies that we have to consider a three degrees-of-freedom (dof) Hamiltonian problem. We know, see for instance

[13] chapter 10 or [18], that the first order resonances are $1 : 2 : 1, 1 : 2 : 2, 1 : 2 : 3$ and $1 : 2 : 4$. The question is then if and how we can choose the masses so that these prominent resonances are present. Of course, this problem will be more formidable if $n > 4$. In the next section we determine for $n = 4$ the ratios of masses that produce the resonance $1 : 2 : 3$. The approach works equally well for other prescribed ratios of eigenvalues, as we discuss in the Appendix. Prominent resonances for $n > 4$ can be found but a systematic study of these cases poses a difficult open algebraic problem.

3 The spectrum induced by H_2

After a number of general considerations we will give details for the cases of three and four particles. The first case is rather trivial as far as the spectrum goes, the case of four particles is already quite complicated. Here we mention the main facts that we need in the later sections. In the Appendix we will give more details.

3.1 The matrix for inhomogeneous FPU-lattices and its eigenvalues

The linear system (3) can be written as

$$\begin{pmatrix} \dot{q} \\ \dot{\tilde{q}} \end{pmatrix} = M \begin{pmatrix} q \\ \tilde{q} \end{pmatrix}, \text{ where } M = \begin{pmatrix} 0 & I_n \\ -A_n C_n & 0 \end{pmatrix}, \quad (5)$$

where the matrix A_n is a diagonal matrix with the inverse masses $m_j^{-1} =: a_j$ on the diagonal, and where the matrix C_n has elements 2 on the diagonal, and -1 at positions $(i, i + 1)$ and $(i, i - 1)$, with the indices taken modulo n . For instance,

$$C_5 = \begin{pmatrix} 2 & -1 & 0 & 0 & -1 \\ -1 & 2 & -1 & 0 & 0 \\ 0 & -1 & 2 & -1 & 0 \\ 0 & 0 & -1 & 2 & -1 \\ -1 & 0 & 0 & -1 & 2 \end{pmatrix}.$$

(This matrix turns up elsewhere in mathematics. It is the affine Cartan matrix of the completed root system \bar{A}_n . See eg. [1, Df. 3 in 1.5 of Chap. 6, and Planche I].)

The $(2n) \times (2n)$ matrix M has a double eigenvalue 0, corresponding to the momentum integral

$$\sum_{j=1}^n m_j \dot{q}_j = \text{constant}. \quad (6)$$

In the sequel we will choose the case of vanishing momentum integral which is not a restriction of generality. If λ is a positive eigenvalue of $A_n C_n$, then $i\sqrt{\lambda}$ and $-i\sqrt{\lambda}$ are eigenvalues of M , corresponding to frequencies of eigenmodes of the linearized system. So it is useful to collect results concerning the eigenvalues of $A_n C_n$.

Proposition 3.1

For $n = 3, 4 \dots$ the matrix $A_n C_n$ has one eigenvalue 0 and $n - 1$ positive eigenvalues $\lambda_1, \dots, \lambda_{n-1}$, possibly coinciding. If eigenvalues coincide the corresponding eigenspace has maximal dimension.

Proof. Since the $a_j = m_j^{-1}$ are positive, the matrix $A_n^{1/2}$ is well-defined. The symmetric matrix $A_n^{1/2} C_n A_n^{1/2}$ has real eigenvalues, and the algebraic and geometric multiplicities of eigenvalues coincide.

If y is an eigenvector of $A_n C_n$ with eigenvalue λ , then

$$\lambda \sum_i a_i^{-1} y_i^2 = 2 \sum_i y_i^2 - 2 \sum_i y_i y_{i-1}.$$

(Indices taken modulo n .) So

$$\sum_i (2 - \lambda/a_i) y_i^2 = 2 \sum_i y_i y_{i-1}.$$

With Schwarz's inequality this implies $\lambda \geq 0$. Equality occurs only if the vectors (y_i) and (y_{i-1}) are positive multiples of each other, which occurs only for multiples of $(1, 1, \dots, 1)$. \square

For the investigation of the linearized problem we need to understand the map $\mathbb{R}_{>0}^n \rightarrow \mathbb{R}_{>0}^{n-1}$, from a vector (a_1, \dots, a_n) of inverse masses to a vector $(\lambda_1, \dots, \lambda_{n-1})$ of positive eigenvalues. The order of the eigenvalues is not determined, so we have, more precisely, a map $\rho_n : \mathbb{R}_{>0}^n \rightarrow S_{n-1} \backslash \mathbb{R}_{>0}^{n-1}$, with the action of the symmetric group S_{n-1} on the coordinates. For the linearized inhomogeneous FPU-chain described by system (3), the dihedral group D_n with $2n$ elements permutes the coordinate q_j (generated by a shift and a reflection). This transforms system (3) into an equivalent system. Another symmetry is by scaling: $\rho(t(a_1, \dots, a_n)) = t \rho(a_1, \dots, a_n)$ for $t > 0$.

To investigate the correspondence between eigenvalues and inverse masses we use the equality

$$\det(A_n C_n - \lambda I_n) = -\lambda \prod (\lambda_j - \lambda),$$

for $(\lambda_1, \dots, \lambda_{n-1}) = \rho(a_1, \dots, a_n)$. This leads to equalities

$$p_j(A_n) = e_{n-j}(\{\lambda_1, \dots, \lambda_{n-1}\}) \quad (1 \leq j \leq n-1), \quad (7)$$

with the elementary symmetric functions e_k and homogeneous polynomials $p_j(A_n)$ in the a_j of degree $n-j$. This describes the structure of the set of diagonal matrices A_n for a prescribed spectrum of $A_n C_n$. It is the set of points with positive coordinates in an algebraic set in \mathbb{C}^n which is the intersection of $n-1$ hyperplanes given by equations of degree $1, 2, \dots, n-1$.

In particular,

$$p_{n-1}(A_n) = 2 \sum_i a_i, \quad p_{n-2}(A_n) = \sum_{1 \leq i < j \leq n} c_{i,j} a_i a_j, \quad (8)$$

with $c_{i,j} = 3$ if $i-j = \pm 1 \pmod n$, and $c_{i,j} = 4$ otherwise. All $p_j(A_n)$ are invariant under the action of the dihedral group D_n on the coordinates a_j .

In subsection A.1 of the Appendix we'll prove relation (8). We will also show that all real solutions (a_1, \dots, a_n) for a given eigenvalue vector $(\lambda_1, \dots, \lambda_{n-1})$ are in a compact subset of \mathbb{R}^n . This subset may be empty. For all $n \geq 4$ the $1 : 1 : \dots : 1$ resonance does not occur for any mass distribution.

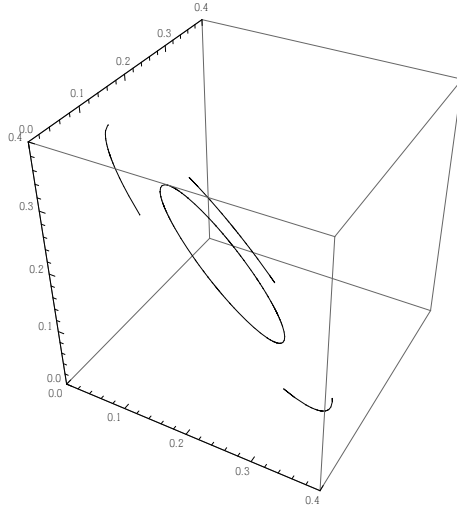


Figure 1: Solutions sets of inverse masses (a_1, a_2, a_3) for the FPU-chain with three particles. For the eigenvalue ratio $\lambda_1/\lambda_2 = 2$ of matrix $A_n C_n$ the solution set is compact; it is an ellipse in $\mathbb{R}_{>0}^3$. For the eigenvalue ratio $\lambda_1/\lambda_2 = 4$ the solutions are on a larger ellipse in \mathbb{R}^3 , which intersects $\mathbb{R}_{>0}^3$ in three open curves.

3.2 The case of three particles

For $n = 3$ the determination of the eigenvalues for given inverse masses amounts to solving the quadratic equation

$$\lambda^2 - 2(a_1 + a_2 + a_3)\lambda + 3(a_1a_2 + a_1a_3 + a_2a_3) = 0,$$

which has positive solutions.

Conversely, for all choices (λ_1, λ_2) of positive eigenvalues, values of a_1, a_2, a_3 can be found such that $A_3 C_3$ has eigenvalues λ_1, λ_2 and 0. If $\lambda_1 = \lambda_2$ there is exactly one solution $a_1 = a_2 = a_3 = \frac{1}{3}\lambda$ (equal masses). If the eigenvalues have ratio $\lambda_1/\lambda_2 > 1$ then the corresponding points (a_1, a_2, a_3) in \mathbb{R}^3 form an ellipse. This ellipse may or may not be contained in the positive octant. See figure 1.

3.3 The case of four particles

In the case $n = 4$ we use the scaling to restrict our further investigation to eigenvalues satisfying $\lambda_1 + \lambda_2 + \lambda_3 = 1$. From (8) we obtain three equations for a given vector $(\lambda_1, \lambda_2, \lambda_3) \in \mathbb{R}_{>0}^3$:

$$\begin{aligned} 4(a_1a_2a_3 + a_2a_3a_4 + a_3a_4a_1 + a_4a_1a_2) &= \lambda_1\lambda_2\lambda_3 =: \zeta, \\ 3(a_1a_2 + a_2a_3 + a_3a_4 + a_4a_1) + 4(a_1a_3 + a_2a_4) &= \lambda_1\lambda_2 + \lambda_2\lambda_3 + \lambda_3\lambda_1 =: \eta, \\ 2(a_1 + a_2 + a_3 + a_4) &= 1. \end{aligned} \quad (9)$$

We call the set of $(a_1, \dots, a_4) \in \mathbb{R}_{>0}^4$ satisfying these relations the *fiber* of $(\zeta, \eta) \in \mathbb{R}_{>0}^2$. In subsection A.1 we will give a precise characterization of the set of (ζ, η) for which the fiber is non-empty.

The resonances deserve special attention. A resonance $(n_1 : n_2 : n_3)$ in the linearized system (3) corresponds to an eigenvalue vector of A_4C_4 with the ratios $(n_1^2 : n_2^2 : n_3^2)$. We considered all resonances of order one and two, and obtained the results in Table 1. As noted in subsection 1.3, the resonances $1 : 1 : 2$ and $1 : 1 : 3$ need special attention.

| ratio | fiber | ratio | fiber |
|-----------------------|---|---------------|--------------------|
| $(1 : 1 : \sqrt{2})$ | one point (classical case $A_4 = I_4$) | | |
| resonances of order 1 | | | |
| $(1 : 1 : 2)$ | four points | $(1 : 2 : 2)$ | empty |
| $(1 : 2 : 3)$ | four open curves | $(1 : 2 : 4)$ | 12 open curves |
| resonances of order 2 | | | |
| $(1 : 1 : 1)$ | empty | $(1 : 1 : 3)$ | four points |
| $(1 : 2 : 5)$ | 12 open curves | $(1 : 2 : 6)$ | 12 open curves |
| $(1 : 3 : 3)$ | empty | $(1 : 3 : 4)$ | four open curves |
| $(1 : 3 : 5)$ | four open curves | $(1 : 3 : 6)$ | 12 open curves |
| $(1 : 3 : 7)$ | 12 open curves | $(1 : 3 : 9)$ | 12 open curves |
| $(2 : 3 : 4)$ | two compact curves | $(2 : 3 : 6)$ | two compact curves |

Table 1: Fibers of resonances

3.4 The resonance $(1 : 2 : 3)$

Here we consider the resonance that is the subject of study in the next section.

By scaling we arrange $\lambda_1 = \frac{9}{14}$, $\lambda_2 = \frac{2}{7}$, $\lambda_3 = \frac{1}{14}$ to satisfy the last equation in (9). The first equation $e_3(\{a_1, a_2, a_3, a_4\}) = \frac{1}{4}\zeta = \frac{9}{2744}$ contains the third elementary symmetric polynomial in the a_j . The middle equation has the form

$$3q_2(a_1, a_2, a_3, a_4) + 4q_1(a_1, a_2, a_3, a_4) = \eta = \frac{1}{4}, \quad (10)$$

with polynomials

$$q_1(a_1, a_2, a_3, a_4) = a_1a_3 + a_2a_4, \quad q_2(a_1, a_2, a_3, a_4) = a_1a_2 + a_2a_3 + a_3a_4 + a_4a_1, \quad (11)$$

which are invariant under the dihedral group D_4 . We solve the system of equations (9) by prescribing values for these two polynomials. So we work with $q_1(a_1, a_2, a_3, a_4) = \eta_1$, $q_2(a_1, a_2, a_3, a_4) = \eta_2$, where η_1 and η_2 satisfy $4\eta_1 + 3\eta_2 = \eta = \frac{1}{4}$. Since both are to be positive this requires $0 < \eta_2 < \frac{1}{12}$.

Now we have four equations for the four unknown quantities a_j , and may expect a discrete set of solutions for each appropriate value of the parameter η_2 .

First we consider the positive quantities $s_{13} = a_1 + a_3$, and $s_{24} = a_2 + a_4$. They satisfy

$$s_{13} + s_{24} = \frac{1}{2}, \quad s_{13}s_{24} = \eta_2.$$

Hence we may take

$$s_{13}, s_{24} = \frac{1}{4} \mp \frac{1}{4} \sqrt{1 - 16\eta_2}. \quad (12)$$

This has positive values only if $0 < \eta_2 < \frac{1}{16}$. In the case of the resonance (1 : 2 : 3) it turns out to be convenient to write $\sqrt{1 - 16\eta_2} = \frac{5-u}{7}$, and to use $u \in (-2, 5]$ as the parameter. We take

$$s_{13} = \frac{1}{4} - \frac{1}{4} \frac{5-u}{7} = \frac{2+u}{28}, \quad s_{24} = \frac{12-u}{28}. \quad (13)$$

For $p_{13} = a_1 a_3$ and $p_{24} = a_2 a_4$ we find the relations

$$p_{13} + p_{24} = \eta_1, \quad s_{13} p_{24} + s_{24} p_{13} = \frac{\xi}{4}.$$

If $u = 5$ we have $s_{13} = s_{14}$. Then $\eta_2 = \frac{1}{16}$, and $\eta_1 = \frac{1}{4} \left(\frac{1}{4} - \frac{3}{16} \right) = \frac{1}{64}$. Since $\xi = \frac{9}{686} \neq \frac{1}{64}$ this does not lead to a solution. So we can proceed with $-2 < u < 5$ and find solutions

$$p_{13} = \frac{\xi/4 - s_{13}\eta_1}{\frac{1}{2}\sqrt{1-16\eta_2}}, \quad p_{24} = \eta_1 - p_{13}. \quad (14)$$

These quantities should be positive. To have $p_{13} > 0$ we need to restrict u to the interval $(0, u_1)$ with

$$u_1 = \frac{8}{3} - \frac{2}{3} \sqrt[3]{19} \approx .887732. \quad (15)$$

Now we have $a_1 + a_3 = s_{13}$ and $a_1 a_3 = p_{13}$. This gives a quadratic equation for a_1 and a_3 , with discriminant

$$\frac{(16-u)(6-u)u}{1568(5-u)}. \quad (16)$$

So there are real solutions that coincide for $u = 0$.

$$a_1, a_3 = \frac{2+u}{56} \mp \frac{\sqrt{2}}{112} \sqrt{\frac{u(6-u)(16-u)}{5-u}}, \quad (17)$$

where we take the minus sign for a_1 . Both functions are positive for $u \in [0, u_1)$. At $u = 0$ they have the same value. The limit $\lim_{u \rightarrow u_1} a_1(u)$ is zero, corresponding to the extreme case of an infinite mass.

The discriminant $s_{24}^2 - 4p_{24}$ of the equation for a_2 and a_4 is positive for all $u \in [0, u_1)$. and leads to two solutions that are unequal for all $u \in [0, u_1)$.

$$a_2, a_4 = \frac{12-u}{56} \mp \frac{1}{56\sqrt{2}} \sqrt{\frac{(6+u)(4-u)(10-u)}{5-u}}, \quad (18)$$

with the minus sign for a_2 . Figure 2 gives a plot.

In the course of the proof we have made three sign choices, in (17) and (18), and in (12). We get all solutions when we let the dihedral group D_4 act on the solutions that we constructed.

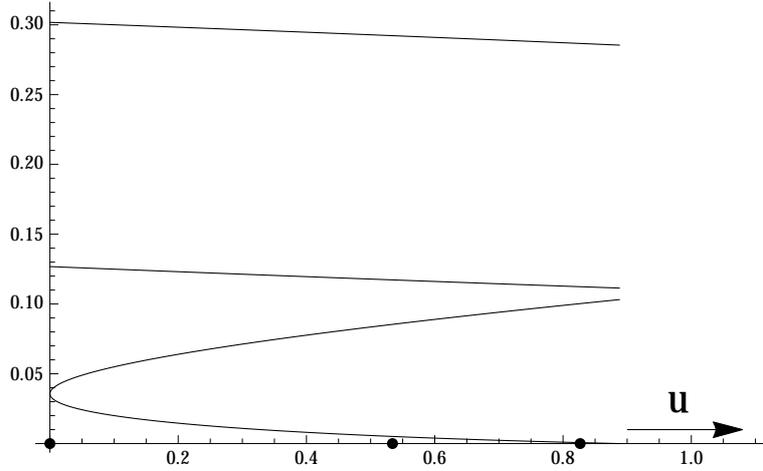


Figure 2: One branch of the fiber for the resonance $(1 : 2 : 3)$ is given by the functions $a_1 \leq a_3 < a_2 < a_4$ on the interval $[0, u_1)$. (Horizontal axis: parameter u ; vertical axis: values of $a_j(u)$.) The three dots on the horizontal axis correspond to the values 0, 0.534105 and 0.826713 of the parameter u for which we will carry out simulations in the next section (the cases 0, 1 and 2).

3.5 Illustration of the fiber

The equations (17) and (18) describe a curve $u \mapsto (a_1(u), a_2(u), a_3(u), a_4(u))$ in $\mathbb{R}_{>0}^4$ corresponding to a one-parameter family of solutions for the inverse masses. To illustrate it we use the second and last equation in (9), which describe an ellipsoid in the hyperplane $a_1 + a_2 + a_3 + a_4 = \frac{1}{2}$. In subsection A.1.1 in the appendix we'll describe this ellipsoid in a more explicit way. The first equation in (9) produces an intersection with this ellipsoid in some curves. The points with positive coordinates in this intersection form the fiber.

On the ellipsoid we can use a system of spherical coordinates, mapping the ellipsoid to the rectangle $[-\pi, \pi] \times [-\frac{1}{2}\pi, \frac{1}{2}\pi]$, with boundary identifications. The image of the fiber under this map is given in figure 3.

3.6 Transformation of the Hamiltonian

We form the diagonal matrix $A_4(u)$ with diagonal elements $a_j(u)$, $1 \leq j \leq 4$. In the proof of Proposition 3.1 we noted that $A_4(u)^{1/2}C_4A_4(u)^{1/2}$ is a symmetric matrix (as long as $u \in [0, u_1)$), so we can find an orthogonal matrix $U(u)$ such that $A_4(u)^{1/2}C_4A_4(u)^{1/2} = U(u)\Lambda U(u)^T$, where Λ is the diagonal matrix with diagonal elements $\frac{9}{14}$, $\frac{2}{7}$, $\frac{1}{14}$, and 0. Then the transformation matrices

$$K(u) = A_4(u)^{-1/2}U(u), \quad L(u) = A_4(u)^{1/2}U(u) \quad (19)$$

determine a symplectic transformation

$$p = K(u)y, \quad q = L(u)x, \quad (20)$$

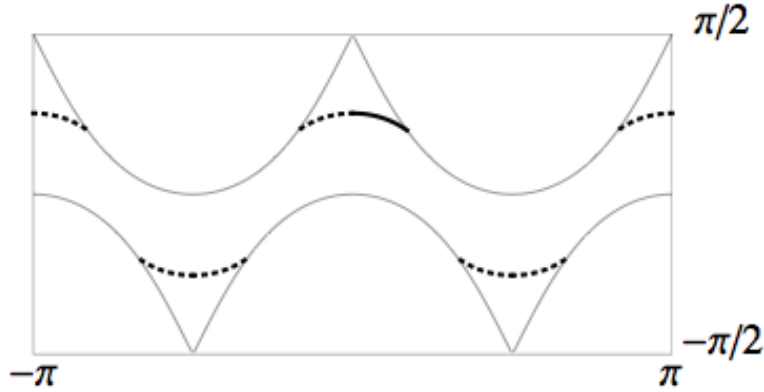


Figure 3: The fiber for the resonance (1 : 2 : 3) is contained in an ellipsoid, which we describe in spherical coordinates. (Horizontally the azimuth ϕ , and vertically the inclination ψ . See (55).) The thick curve corresponds to the branch of the fiber in figure 2. The dotted curves correspond to the translates of this branch under the dihedral group D_4 . The thin curves indicate the boundary of the region corresponding to coordinates in $\mathbb{R}_{>0}^4$. The picture illustrates that the fiber for (1 : 2 : 3) consists of four open curves, and that (17) and (18) give a fundamental domain for the action of the dihedral group on the fiber.

which transforms the quadratic part in (4) of the Hamiltonian into

$$H_2 = \frac{1}{2}y^T y + \frac{1}{2}x^T \Lambda x = \frac{1}{2} \sum_{j=1}^4 (y_j^2 + \lambda_j x_j^2). \quad (21)$$

This will produce the so-called quasi-harmonic form of the equations of motion. To see that H_2 takes the form (21) we need the existence of an orthogonal matrix $U(u)$ diagonalizing $A_4(u)^{1/2} C_4 A_4(u)^{1/2}$. We do not need to know $U(u)$, $K(u)$ or $L(u)$ explicitly.

To transform the cubic and higher order terms of the Hamiltonian to coordinates corresponding to the eigenmodes of the linearized system we need to know the transformation matrix $L(u)$ explicitly. For any given $u \in [0, u_1]$ it is no problem to do this numerically with MATHEMATICA or MATLAB. It is nicer to have $U(u)$, and hence $L(u)$ and $K(u)$, symbolically in terms of the parameter u ; see subsection A.4. The explicit description of our choice of $L(u)$ will be given in Table 4 in the appendix.

For the cubic term we note that (with indices modulo 4)

$$\frac{1}{3} \sum_j (q_{j+1} - q_j)^3 = \sum_j (q_{j+1} - q_{j-1}) q_j^2. \quad (22)$$

The substitution $(q_1, \dots, q_4)^T = L(u)(x_1, \dots, x_4)^T$ gives

$$H_3 = \varepsilon (d_1(u)x_1^3 + d_2(u)x_1^2 x_2 + d_3(u)x_1^2 x_3 + d_4(u)x_2^2 x_1 + d_5(u)x_3^2 x_1 + d_6(u)x_1 x_2 x_3 + d_7(u)x_2^3 + d_8(u)x_3^3 + d_9(u)x_3^2 x_2 + d_{10}(u)x_2^2 x_3), \quad (23)$$

with the functions d_j as indicated in Table 2.

$$\begin{aligned}
d_1(u) &= \sqrt{u} \frac{27\sqrt{4-u}\sqrt{6-u}\sqrt{10-u}(16-u)(u+6)}{35840\sqrt{35}(5-u)}, \\
d_2(u) &= -\sqrt{u} \frac{3\sqrt{3}\sqrt{10-u}\sqrt{16-u}\sqrt{u+6}(3u^2-30u+52)}{4480\sqrt{70}(5-u)}, \\
d_3(u) &= -\frac{3\sqrt{3}\sqrt{4-u}\sqrt{6-u}\sqrt{16-u}\sqrt{u+6}(3u^2-30u+160)}{35840\sqrt{7}(5-u)}, \\
d_4(u) &= -\sqrt{u} \frac{\sqrt{4-u}\sqrt{6-u}\sqrt{10-u}(-3u^2+30u+68)}{1120\sqrt{35}(5-u)}, \\
d_5(u) &= -\sqrt{u} \frac{\sqrt{4-u}\sqrt{6-u}\sqrt{10-u}(3u^2-30u+64)}{7168\sqrt{35}(5-u)}, \\
d_6(u) &= -\frac{-3u^4+60u^3-352u^2+520u+960}{2240\sqrt{14}(5-u)}, \\
d_7(u) &= \sqrt{u} \frac{\sqrt{10-u}\sqrt{16-u}(6-u)(4-u)\sqrt{u+6}}{420\sqrt{210}(5-u)}, \\
d_8(u) &= u \frac{\sqrt{4-u}\sqrt{6-u}\sqrt{16-u}(10-u)\sqrt{u+6}}{21504\sqrt{21}(5-u)}, \\
d_9(u) &= -\sqrt{u} \frac{\sqrt{10-u}\sqrt{16-u}\sqrt{u+6}(u^2-10u+28)}{869\sqrt{210}(5-u)}, \\
d_{10}(u) &= \frac{\sqrt{4-u}\sqrt{6-u}\sqrt{16-u}\sqrt{u+6}(u^2-10u+20)}{1120\sqrt{21}(5-u)}.
\end{aligned}$$

Table 2: Coefficients of the cubic term of the Hamiltonian, transformed to eigenmodes, the so-called quasi-harmonic form. For $u = 0$ only d_3 , d_6 and d_{10} are non-zero.

4 The 1 : 2 : 3-resonance for the periodic α -lattice ($n = 4$)

For any possible inhomogeneous FPU α -chain with four dof we have the system:

$$\begin{cases} \dot{q}_1 = v_1, \\ \dot{v}_1 = [-2q_1 + q_2 + q_4 - \varepsilon\alpha((q_1 - q_4)^2 - (q_2 - q_1)^2)]a_1, \\ \dot{q}_2 = v_2, \\ \dot{v}_2 = [-2q_2 + q_3 + q_1 - \varepsilon\alpha((q_2 - q_1)^2 - (q_3 - q_2)^2)]a_2, \\ \dot{q}_3 = v_3, \\ \dot{v}_3 = [-2q_3 + q_4 + q_2 - \varepsilon\alpha((q_3 - q_2)^2 - (q_4 - q_3)^2)]a_3, \\ \dot{q}_4 = v_4, \\ \dot{v}_4 = [-2q_4 + q_1 + q_3 - \varepsilon\alpha((q_4 - q_3)^2 - (q_1 - q_4)^2)]a_4, \end{cases} \quad (24)$$

The coefficient α has been retained for reference to the literature; here we will take $\alpha = 1$. If $a_1 = \dots = a_4 = 1$, we have the classical periodic FPU problem with four particles; it was shown in [11], that in this case the normal form is integrable. The implication is that for ε small, chaos is negligible in this classical case.

Apart from the Hamiltonian we have from (6) as a second (momentum) integral:

$$m_1v_1 + m_2v_2 + m_3v_3 + m_4v_4 = \text{constant}. \quad (25)$$

The presence of the momentum integral results in two zero eigenvalues of the matrix M in eq. (5), so by reduction we have to deal essentially with a three dof system.

According to table 1 the 1 : 2 : 3 resonance is present among the possible inhomogeneous FPU lattices. Fig. 2 gives one branch of values of inverse masses a_1, \dots, a_4 producing this resonance. All vectors (a_1, \dots, a_4) are obtained by the action of the dihedral group D_4 on the coordinates and the scaling $(a_1, \dots, a_4) \mapsto (ta_1, \dots, ta_4)$ with $t > 0$.

Table 1 and fig. 2 show that the 1 : 2 : 3 -resonance appears in one case with relatively well-balanced masses, two of which are equal. We denote this by case 0; it will turn out in subsection 4.1 that this case is quite special dynamically. The other cases are less balanced regarding the masses. Case 0 corresponds to $u = 0$; as u increases (we have $0 \leq u < u_1$ with $u_1 = .887732$), the masses get less well-balanced, one of them tending to infinity. We study the dynamical behaviour in subsection 4.2. For numerical simulations we have singled out two more cases indicated in fig. 2.

The expression for the quadratic part of the Hamiltonian H_2 is:

$$H_2 = \frac{1}{2} \sum_{i=1}^4 \frac{v_i^2}{a_i} + \frac{1}{2} [(q_2 - q_1)^2 + (q_3 - q_2)^2 + (q_4 - q_3)^2 + (q_1 - q_4)^2]. \quad (26)$$

H_2 is a first integral of the linear system (3), it is also a first integral of the normal form of the full system (24). When using H_2 from the solutions of the truncated normal form

$$\bar{H}(p, q) = H_2(p, q) + \varepsilon \bar{H}_3(p, q),$$

we obtain an $O(\varepsilon)$ approximation of the (exact) $H_2(p(t), q(t))$ valid for all time; for a proof see [13] chapter 10. Note that in the equations we use the velocities instead of the momenta.

Using the expression $H_2(p(t), q(t))$ for the solutions of the full system (24) shows the accuracy of the normal form and gives an impression of the nature of the dynamics.

The normal form $\bar{H}_3(p, q)$, written in action-angle coordinates (1) or amplitude-phase coordinates (see below), will contain certain combination angles corresponding with the resonance. If \bar{H}_3 contains only one combination angle, we have an additional integral of motion and the normal form $H_2 + \bar{H}_3$ is integrable. In the case of two or more independent combination angles, we have to investigate the (non-)integrability of the normal form.

To display the quantitative aspects of the solutions we have the possibility of drawing an energy- or action-simplex or as an alternative to produce a time series for explicit solutions or integrals of the normal forms. Both techniques will be used.

As the short-periodic solutions have constant actions (or constant radii in polar coordinates), the integral H_2 of the normal form produces for fixed energy an action-simplex with short-periodic solutions represented by points; the actions τ_i and the polar coordinates r_i are related by the transformations (1) and (31). One way of displaying the position of short-periodic solutions and their stability on the 5-dimensional energy manifold is the use of this action-simplex with normal modes at the vertices and solutions in the coordinate planes at the sides. The interior of the faces may contain short-periodic solutions in general position. Their stability is indicated by E (elliptic i.e. imaginary eigenvalues), H (hyperbolic i.e. real eigenvalues) and C (complex eigenvalues with real parts non-zero). See for instance for the action simplices displaying periodic solutions fig. 6.

4.1 Case 0: the FPU problem with well-balanced masses

In this case we have the 1 : 2 : 3 resonance with mass values that are as much as possible similar; we have with $u = 0$ in (17) and (18):

$$a_1 = 0.0357143, a_2 = 0.126804, a_3 = 0.0357143, a_4 = 0.301767.$$

Note that $a_1 = a_3$. We checked numerically that the time series $H_2(p(t), q(t))$ based on the original formulation of system (24) and the time series obtained from the transformed Hamiltonian (27) produce the same result as it should.

To put system (24) in the standard form of quasi-harmonic equations we have to apply the symplectic transformation $p = K(0)y, q = L(0)x$ in (20). This leads with (23) and table 2 to the transformed Hamiltonian

$$H(y, x) = \frac{1}{2} \sum_{i=1}^4 (y_i^2 + \omega_i^2 x_i^2) + \varepsilon (d_3 x_1^2 + d_{10} x_2^2 + d_6 x_1 x_2) x_3, \quad (27)$$

with

$$\omega_1^2 = \frac{9}{14}, \omega_2^2 = \frac{4}{14}, \omega_3^2 = \frac{1}{14}, \omega_4^2 = 0, d_3 = -9 \frac{\sqrt{21}}{490}, d_{10} = 2 \frac{\sqrt{21}}{245}, d_6 = -3 \frac{\sqrt{14}}{490}.$$

Rescaling time $t/\sqrt{14} \rightarrow t$, the equations of motion for the three dof system become:

$$\begin{cases} \ddot{x}_1 + 9x_1 &= -\varepsilon 14(2d_3 x_1 x_3 + d_6 x_2 x_3), \\ \ddot{x}_2 + 4x_2 &= -\varepsilon 14(2d_{10} x_2 x_3 + d_6 x_1 x_3), \\ \ddot{x}_3 + x_3 &= -\varepsilon 14(d_3 x_1^2 + d_{10} x_2^2 + d_6 x_1 x_2). \end{cases} \quad (28)$$

According to the Weinstein [19] result there exist at least three families of short-periodic solutions of system (28). Inspection of the equations provides us directly with one family given by:

$$x_1(t) = \dot{x}_1(t) = x_2(t) = \dot{x}_2(t) = 0, \quad \ddot{x}_3 + x_3 = 0. \quad (29)$$

For fixed energy we refer to this periodic solution as the x_3 normal mode; to find such an exact solution explicitly is slightly unusual, the solution is harmonic. Additional periodic solutions are obtained as approximations from normal forms as in [8]. In general, when normalizing a three dof system, one recovers the three actions (introduced in (1)) and one expects to find the angles in combinations according to the actual resonances. For the 3 : 2 : 1 resonance these are to first order after normalization the so-called combination angles $\phi_1 - \phi_2 - \phi_3$ and $2\phi_3 - \phi_2$. At second order the combination angle $\phi_1 - 3\phi_3$ will arise etc., for details see section 10.2.1 of [13]; for instance the term ‘genuine resonance’ associated with the so-called ‘annihilators’ of H_2 can be found in definition 10.2.2 of [13].

Computing the normal form of system (28) to $O(\varepsilon)$ ($H_2 + \varepsilon\bar{H}_3$) as in [8] or [13] and as we shall explicitly show below, only the d_6 term survives in \bar{H}_3 ; this makes the Hamiltonian (27) non-generic. An *intermediate normal form* of the equations of motion becomes:

$$\begin{cases} \ddot{x}_1 + 9x_1 &= -\varepsilon 14d_6 x_2 x_3, \\ \ddot{x}_2 + 4x_2 &= -\varepsilon 14d_6 x_1 x_3, \\ \ddot{x}_3 + x_3 &= -\varepsilon 14d_6 x_1 x_2. \end{cases} \quad (30)$$

As discussed in the Introduction, there is a lot of freedom in choosing coordinate systems to compute the normal form of the equations of motion. Near the coordinate planes, in particular to study the stability of the normal modes, we will use co-moving coordinates. Away from the coordinate planes (solutions in general position), action-angle variables or polar coordinates are easier to handle than co-moving coordinates. Some authors frown upon the use of polar coordinates anyway, because they do not conserve the canonical character of the normal forms; however, they preserve the energy and as normal forms they still present a mathematical precise normal form approximation of the solutions. For general position orbits we will use in system (28) transformations $x_i, \dot{x}_i \rightarrow r_i, \psi_i$ of the form:

$$x_i = r_i \cos(\omega_i t + \psi_i), \quad \dot{x}_i = -r_i \omega_i \sin(\omega_i t + \psi_i). \quad (31)$$

The actions τ_i are related to the r_i^2 , the angles ϕ_i to the arguments $(\omega_i t + \psi_i)$. Putting $\chi = \psi_1 - \psi_2 - \psi_3$ and averaging over time t , the averaging-normal form equations outside the coordinate planes become:

$$\begin{cases} \dot{r}_1 &= \varepsilon \frac{7}{6} d_6 r_2 r_3 \sin \chi, \\ \dot{r}_2 &= -\varepsilon \frac{7}{4} d_6 r_1 r_3 \sin \chi, \\ \dot{r}_3 &= -\varepsilon \frac{7}{2} d_6 r_1 r_2 \sin \chi, \\ \dot{\chi} &= \varepsilon \frac{7}{2} d_6 \frac{\cos \chi}{r_1 r_2 r_3} \left(\frac{r_2^2 r_3^2}{3} - \frac{r_1^2 r_3^2}{2} - \frac{r_1^2 r_2^2}{1} \right). \end{cases} \quad (32)$$

The integral H_2 of the normal form equations becomes:

$$9r_1^2 + 4r_2^2 + r_3^2 = 2E_0, \quad (33)$$

with E_0 a positive (energy) constant. The combination angle $2\phi_3 - \phi_2$ is missing; another integral of the normal form (32) is:

$$2r_2^2 - r_3^2 = C \text{ (constant)}. \quad (34)$$

In the original variables this integral is:

$$2x_2^2 + \frac{1}{2}\dot{x}_2^2 - x_3^2 - \dot{x}_3^2 = \text{constant}.$$

As we have three independent integrals of the normal form equations (32), the normal form is integrable. Because of the approximative character of the normal form, this means that chaotic motion in the original system (28) is restricted to $O(\varepsilon)$.

Periodic solutions in general position exist if $\sin \chi = 0, t \geq 0$ for certain values of the r_i . From the 4th equation of system (32) we find the requirement:

$$\frac{r_2^2 r_3^2}{3} - \frac{r_1^2 r_3^2}{2} - \frac{r_1^2 r_2^2}{1} = 0.$$

Eliminating r_1 by the H_2 integral we find after some rearrangements the condition

$$2r_2^2 r_3^2 + \frac{4}{3}r_2^4 + \frac{1}{6}r_3^4 = \frac{1}{3}E_0(2r_2^2 + r_3^2), \quad 0 < r_2 < \sqrt{\frac{E_0}{2}}, \quad 0 < r_3 < \sqrt{2E_0}. \quad (35)$$

Both for $\chi = 0$ and for $\chi = \pi$ we find from condition (35) tori imbedded in the energy manifold. The two tori consist of periodic solutions in general position connecting the x_2 and x_3 normal modes. Their period is $O(\varepsilon)$ modulated by their position on the tori. The relation between the presence of a continuous family of periodic solutions on the energy manifold and the existence of another integral (34) is an example of a more general theory on characteristic exponents of periodic solutions developed by Poincaré in [10], vol. 1.

Periodic solutions in the coordinate planes

It is clear from the intermediate normal form (30) that the normalized equations of motion will contain all three normal modes. We will use co-moving coordinates to study the stability:

$$\begin{cases} x_1 = y_1 \cos 3t + \frac{1}{3}y_2 \sin 3t, \dot{x}_1 = -3y_1 \sin 3t + y_2 \cos 3t, \\ x_2 = z_1 \cos 2t + \frac{1}{2}z_2 \sin 2t, \dot{x}_2 = -2z_1 \sin 2t + z_2 \cos 2t, \\ x_3 = u_1 \cos t + u_2 \sin t, \dot{x}_3 = -u_1 \sin t + u_2 \cos t. \end{cases} \quad (36)$$

The normalized variables are obtained by averaging over time t and are satisfying the system:

$$\begin{cases} \dot{y}_1 = \varepsilon \frac{7}{6} d_6 (z_1 u_2 + \frac{1}{2} z_2 u_1), \\ \dot{y}_2 = -\varepsilon \frac{7}{2} d_6 (z_1 u_1 - \frac{1}{2} z_2 u_2), \\ \dot{z}_1 = \varepsilon \frac{7}{4} d_6 (-y_1 u_2 + \frac{1}{3} y_2 u_1), \\ \dot{z}_2 = -\varepsilon \frac{7}{2} d_6 (y_1 u_1 + \frac{1}{3} y_2 u_2), \\ \dot{u}_1 = \varepsilon \frac{7}{2} d_6 (-\frac{1}{2} y_1 z_2 + \frac{1}{3} y_2 z_1), \\ \dot{u}_2 = -\varepsilon \frac{7}{2} d_6 (y_1 z_1 + \frac{1}{6} y_2 z_2). \end{cases} \quad (37)$$

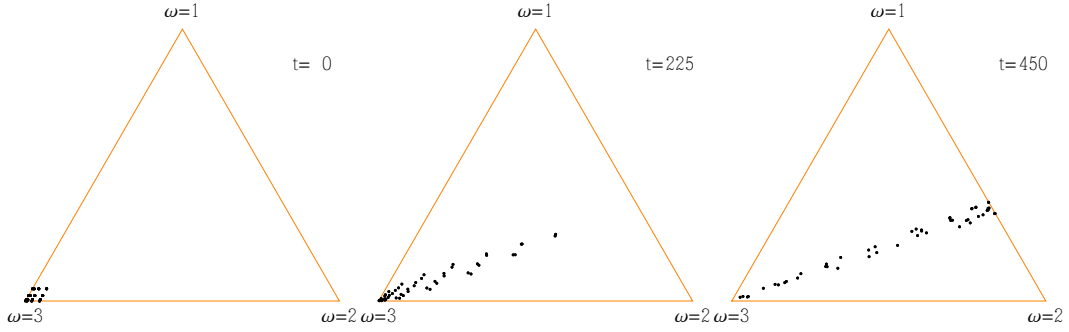


Figure 4: The $\omega = 3$ normal mode (x_1) exists in the case 0 and is unstable (see also fig. 6). We consider the time evolution of 98 initial positions near this normal mode by displaying the actions in the action-simplex at $t = 0, 225, 450$. The evolution is based on Hamiltonian (27); $\varepsilon = 0.2$. The unstable manifold is two-dimensional after which the action points remain near a line in the action simplex. The inclination is explained by the expression of the third integral (34) of the normal form.

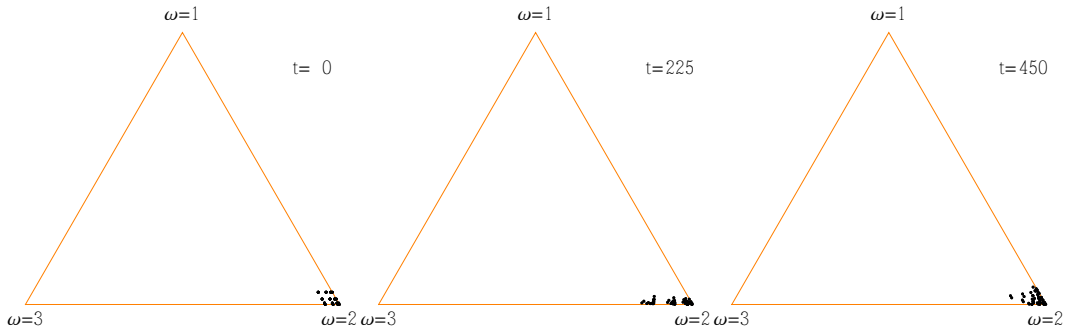


Figure 5: The $\omega = 2$ normal mode (x_2) is stable in the case 0. We consider the time evolution based on Hamiltonian (27) of 98 initial positions near this normal mode by displaying the actions in the action-simplex at $t = 0, 225, 450$; $\varepsilon = 0.2$.

The generic picture for the existence of short-periodic solutions in the Hamiltonian 1 : 2 : 3 resonance is given in [8]. As stated above we recover three normal modes instead of generically two; this is caused by the already mentioned degenerate form of Hamiltonian (27).

The three normal modes of the normalized system are harmonic functions:

$$A \cos mt + B \sin mt, \quad m = 3, 2, 1, \quad A^2 + B^2 > 0.$$

To study their stability we linearize around the normal modes to obtain coupled Mathieu equations; we approximate the characteristic exponents by normalizing these coupled systems. We find:

1. Normal mode x_1 : put $x_1 = A \cos 3t + B \sin 3t + w_1, x_2 = w_2, x_3 = w_3$.

Transforming in the linearized system by (36) and normalization we find:

$$\begin{aligned} \dot{z}_1 &= -\varepsilon \frac{7}{4} d_6 (Bu_1 - Au_2), \\ \dot{z}_2 &= \varepsilon \frac{7}{2} d_6 (Au_1 + Bu_2), \\ \dot{u}_1 &= -\varepsilon \frac{7}{2} d_6 (Bz_1 - \frac{1}{2} Az_2), \\ \dot{u}_2 &= \varepsilon \frac{7}{2} d_6 (Az_1 + \frac{1}{2} Bz_2). \end{aligned}$$

The eigenvalues of the matrix describing this linear system have multiplicity 2 and are multiples of:

$$\pm \sqrt{A^2 + B^2}.$$

In the nomenclature of [13] section 10.7.3 this is the unstable case HH.

It is interesting to consider the action-simplex with a number of initial conditions near the x_1 normal mode, see fig. 4. The unstable manifold of the normal mode is two-dimensional but the solutions, displayed by dots in the simplex, remain in a narrow strip extending to the edge where $x_1 = 0$. This is caused by the third integral (34) of the normal form which tells us that the action corresponding with x_1 is proportional to the action of x_2 .

2. Normal mode x_2 : put $x_1 = w_1, x_2 = A \cos 2t + B \sin 2t + w_2, x_3 = w_3$.

Transforming in the linearized system by (36) and normalization by averaging we find:

$$\begin{aligned} \dot{y}_1 &= -\varepsilon \frac{7}{6} d_6 (Bu_1 + Au_2), \\ \dot{y}_2 &= \varepsilon \frac{7}{2} d_6 (Au_1 - Bu_2), \\ \dot{u}_1 &= \varepsilon \frac{7}{2} d_6 (By_1 - \frac{1}{3} Ay_2), \\ \dot{u}_2 &= \varepsilon \frac{7}{2} d_6 (Ay_1 + \frac{1}{3} By_2). \end{aligned}$$

The eigenvalues have multiplicity 2 and are multiples of:

$$\pm i \sqrt{A^2 + B^2}.$$

In the nomenclature of [13] this is the marginally stable case EE, but with both positive and negative imaginary eigenvalues coincident. A numerical calculation confirms the stability in the sense that the solutions remain near the normal mode during a finite time.

When varying u , this will produce a Hamiltonian-Hopf bifurcation, see the next subsection. As the normal mode is marginally stable, it is of interest to display the behaviour of the actions of solutions starting near this normal mode. In fig. 5 we show that for a limited time interval, the actions stay nearby.

3. Normal mode x_3 : put $x_1 = w_1, x_2 = w_2, x_3 = A \cos t + B \sin t + w_3$.

Transforming in the linearized system by (36) and normalization we find:

$$\begin{aligned} \dot{y}_1 &= -\varepsilon \frac{7}{6} d_6 (Bz_1 + \frac{1}{2} Az_2), \\ \dot{y}_2 &= \varepsilon \frac{7}{2} d_6 (Az_1 - \frac{1}{2} Bz_2), \\ \dot{z}_1 &= \varepsilon \frac{7}{4} d_6 (By_1 - \frac{1}{3} Ay_2), \\ \dot{z}_2 &= \varepsilon \frac{7}{2} d_6 (Ay_1 + \frac{1}{3} By_2). \end{aligned}$$

The eigenvalues have multiplicity 2 and are multiples of:

$$\pm i \sqrt{A^2 + B^2}.$$

In the nomenclature of [13] section 10.7.3, this is the marginally stable case EE, but again with both positive and negative imaginary eigenvalues coincident. The numerical behaviour (not shown) looks similar to fig. 5.

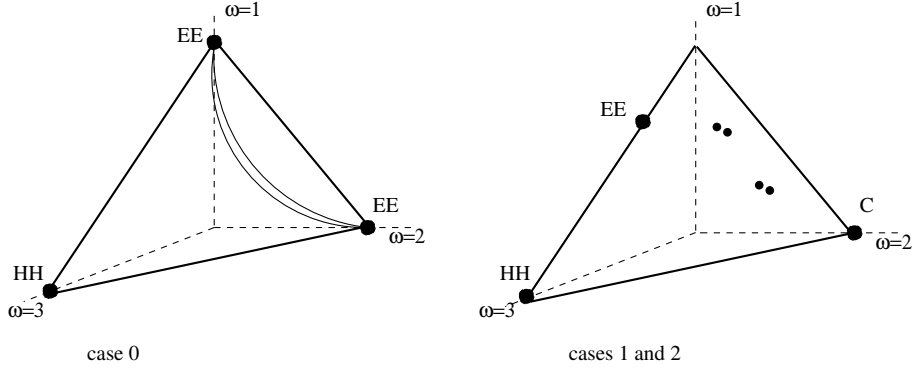


Figure 6: The action simplices of the cases 0, 1 and 2; the cases 1 and 2 are typical for the family of Hamiltonians where $0 < u < u_1$. The actions τ_i (related to r_i^2) form a triangle for fixed values of H_2 which is an integral of the normal forms. The frequencies have been normalized to 1, 2, 3 to indicate the x_3, x_2, x_1 normal mode positions at the vertices. The black dots indicate periodic solutions, the indicated stability types are HH (hyperbolic-hyperbolic), EE (elliptic-elliptic) and C (complex). The two (roughly sketched) curves connecting the x_2 and x_3 normal modes in the left simplex correspond with two tori consisting of periodic solutions, respectively with combination angles $\chi = 0$ and π . The tori break up into 4 general position periodic solutions if $u > 0$ (cases 1 and 2).

Our choice of well-balanced masses involves the symmetry $a_1 = a_3$. In the sequel we will see that other choices of masses producing 1 : 2 : 3 resonance give qualitatively different results. It is interesting to compare the dynamics of case 0 ($u = d_9 = 0$) with the dynamics for $u > 0$. Such a comparison will be given in the next subsections.

4.2 The Hamiltonian-Hopf bifurcation

In the preceding subsection we considered a rather symmetric case, $a_1 = a_3$, corresponding with $u = 0$, producing an integrable normal form; see subsection 3.6 and table 2. We will now consider the cases $0 < u < u_1 (= 0.887732 \dots)$; as u increases through the interval $(0, u_1)$ the masses will differ more and more, producing generic Hamiltonians. To put system (24) in the standard form of perturbed harmonic equations we have to apply again a symplectic transformation, i.e. (20) from subsection 3.6. This leads to a transformed Hamiltonian (with rescaled frequencies) of the form $H_2 + \varepsilon H_3$ with

$$H_2 = \frac{1}{2}(\dot{x}_1^2 + \frac{9}{14}x_1^2 + \dot{x}_2^2 + \frac{4}{14}x_2^2 + \dot{x}_3^2 + \frac{1}{14}x_3^2)$$

and

$$\begin{cases} H_3 = & d_1x_1^3 + d_2x_2x_1^2 + d_3x_3x_1^2 + d_4x_2^2x_1 + d_5x_3^2x_1 + d_6x_1x_2x_3 + d_7x_2^3 + d_8x_3^3 + \\ & d_9x_2x_3^2 + d_{10}x_2^2x_3, \end{cases} \quad (38)$$

with all coefficients non-zero, see table 2. After rescaling time $t \rightarrow t/\sqrt{14}$, the equations of motion for the three dof system can be written as:

$$\begin{cases} \ddot{x}_1 + 9x_1 &= -\varepsilon 14(3d_1x_1^2 + 2d_2x_1x_2 + 2d_3x_1x_3 + d_4x_2^2 + d_5x_3^2 + d_6x_2x_3), \\ \ddot{x}_2 + 4x_2 &= -\varepsilon 14(d_2x_1^2 + 2d_4x_2x_1 + d_6x_1x_3 + 3d_7x_2^2 + d_9x_3^2 + 2d_{10}x_2x_3), \\ \ddot{x}_3 + x_3 &= -\varepsilon 14(d_3x_1^2 + 2d_5x_3x_1 + d_6x_1x_2 + 3d_8x_3^2 + 2d_9x_2x_3 + d_{10}x_2^2). \end{cases} \quad (39)$$

The size of the coefficients of H_3 are comparable with the size of d_6 or smaller, we will give them explicitly as examples for the cases 1 and 2 in subsection 4.3 with less balanced masses.

In the cubic part of the normalized Hamiltonian we retain of the cubic part only the terms with d_6 and d_9 ; the other terms are, after normalization, active only at higher order. So, anticipating this, an intermediate normal form of the equations of motion becomes:

$$\begin{cases} \ddot{x}_1 + 9x_1 &= -\varepsilon 14d_6x_2x_3, \\ \ddot{x}_2 + 4x_2 &= -\varepsilon 14(d_6x_1x_3 + d_9x_3^2), \\ \ddot{x}_3 + x_3 &= -\varepsilon 14(d_6x_1x_2 + 2d_9x_2x_3), \end{cases} \quad (40)$$

The normal form and periodic solutions outside the coordinate planes

Using transformation (31) and putting $\phi_1 - \phi_2 - \phi_3 = \chi_1$, $2\phi_3 - \phi_2 = \chi_2$, we find after averaging-normalization:

$$\begin{cases} \dot{r}_1 &= \varepsilon \frac{7}{6} d_6 r_2 r_3 \sin \chi_1, \\ \dot{r}_2 &= -\varepsilon \frac{7}{4} (d_6 r_1 r_3 \sin \chi_1 + d_9 r_3^2 \sin \chi_2), \\ \dot{r}_3 &= -\varepsilon \frac{7}{2} (d_6 r_1 r_2 \sin \chi_1 - 2d_9 r_2 r_3 \sin \chi_2), \\ \dot{\chi}_1 &= \varepsilon \frac{7}{2} \left[d_6 \frac{\cos \chi_1}{r_1 r_2 r_3} \left(\frac{r_2^2 r_3^2}{3} - \frac{r_1^2 r_3^2}{2} - \frac{r_1^2 r_2^2}{1} \right) - d_9 \frac{\cos \chi_2}{r_2} \left(\frac{1}{2} r_3^2 + 2r_2^2 \right) \right], \\ \dot{\chi}_2 &= \varepsilon \frac{7}{4} \left(d_6 \frac{r_1 \cos \chi_1}{r_2 r_3} (4r_2^2 - r_3^2) + d_9 \frac{\cos \chi_2}{r_2} (8r_2^2 - r_3^2) \right). \end{cases} \quad (41)$$

The integral H_2 of the normal form equations becomes again:

$$9r_1^2 + 4r_2^2 + r_3^2 = 2E_0, \quad (42)$$

Periodic solutions in general position with constant amplitude have to satisfy $\sin \chi_1 = \sin \chi_2 = 0$ or $\chi_1 = 0, \pi$ and $\chi_2 = 0, \pi$. We have

$$\cos \chi_1 \cos \chi_2 = \pm 1, \quad q = \frac{d_9}{d_6} > 0.$$

From the last two equations of system (41) we have the conditions:

$$\frac{r_2^2 r_3^2}{3} - \frac{r_1^2 r_3^2}{2} - \frac{r_1^2 r_2^2}{1} = \pm q r_1 r_3 \left(\frac{1}{2} r_3^2 + 2r_2^2 \right), \quad (43)$$

$$4r_2^2 - r_3^2 = \pm q \frac{r_3}{r_1} (r_3^2 - 8r_2^2). \quad (44)$$

Eliminating r_1 from (43) using (44) we obtain two equations that are quadratic in r_2^2 and r_3^2 . Eliminating r_1 from the H_2 integral we find one equation that is quadratic in r_2^2 and r_3^2 . These expressions have to be handled for the range of q determined by $u \in (0, u_1)$. Using

MATHEMATICA and corresponding plots we find four positive solutions corresponding with four periodic solutions characterized by two different phases.

We omit the stability analysis, but note that the generic case of the 1 : 2 : 3 resonance was studied in [8] that produces four general position periodic solutions with the stability types EE and EH .

Periodic solutions in the coordinate planes

Inspection of the intermediate normal form system (40) shows that the x_1 and x_2 normal modes exist as solutions of this system, the x_3 normal mode does not. It is shown in [8] that the normal mode x_2 is unstable. If the instability is of class C (complex eigenvalues), a Shilnikov-Devaney bifurcation [3] may take place resulting in chaotic dynamics originating from a neighborhood of the complex unstable normal mode. To avoid singularities near the normal modes we use again the co-moving variables from transformation (36). The normalized variables satisfy the system:

$$\begin{cases} \dot{y}_1 &= \varepsilon \frac{7}{6} d_6 (z_1 u_2 + \frac{1}{2} z_2 u_1), \\ \dot{y}_2 &= -\varepsilon \frac{7}{2} d_6 (z_1 u_1 - \frac{1}{2} z_2 u_2), \\ \dot{z}_1 &= \varepsilon \frac{7}{2} [\frac{1}{2} d_6 (-y_1 u_2 + \frac{1}{3} y_2 u_1) + d_9 u_1 u_2], \\ \dot{z}_2 &= -\varepsilon \frac{7}{2} [d_6 (y_1 u_1 + \frac{1}{3} y_2 u_2) + d_9 (u_1^2 - u_2^2)], \\ \dot{u}_1 &= \varepsilon \frac{7}{2} [d_6 (-\frac{1}{2} y_1 z_2 + \frac{1}{3} y_2 z_1) + d_9 (-2z_1 u_2 + z_2 u_1)], \\ \dot{u}_2 &= -\varepsilon \frac{7}{2} [d_6 (y_1 z_1 + \frac{1}{6} y_2 z_2) + d_9 (2z_1 u_1 + z_2 u_2)]. \end{cases} \quad (45)$$

We find three families of short-periodic solutions; the constants A, B are real, $A^2 + B^2 > 0$.

1. $x_1(t) = A \cos 3t + B \sin 3t, x_2 = x_3 = 0$.
2. $x_2(t) = A \cos 2t + B \sin 2t, x_1 = x_3 = 0$.
3. If $x_2(t) = 0, d_6 \neq 0$:

$$\begin{cases} x_1(t) &= \frac{d_9}{d_6} \left(\frac{A}{A^2+B^2} (3B^2 - A^2) \cos 3t - \frac{B}{A^2+B^2} (3A^2 - B^2) \sin 3t \right), \\ x_3(t) &= A \cos t + B \sin t. \end{cases} \quad (46)$$

If d_9 differs from zero, this family of periodic solutions moves along the $x_2 = 0$ edge of the simplex in fig. 6 starting from the x_3 normal mode that exists if $d_9 = 0$.

To evaluate the stability of the periodic solutions we will linearize system (40) near these solutions; this produces coupled Mathieu equations which we will analyze by normalization.

The x_2 normal mode

Put:

$$x_1 = w_1, x_2 = A \cos 2t + B \sin 2t + w_2, x_3 = w_3,$$

with real constants $A, B, A^2 + B^2 > 0$ and corresponding expressions for the derivatives. We find after linearization

$$\begin{cases} \ddot{w}_1 + 9w_1 &= -\varepsilon 14 d_6 (A \cos 2t + B \sin 2t) w_3, \\ \ddot{w}_2 + 4w_2 &= 0, \\ \ddot{w}_3 + w_3 &= -\varepsilon 14 [d_6 w_1 (A \cos 2t + B \sin 2t) + 2d_9 (A \cos 2t + B \sin 2t) w_3], \end{cases} \quad (47)$$

We study the stability of this system by normalization to find the eigenvalues of the matrix (omitting the factor $7\varepsilon/2$)

$$\begin{pmatrix} 0 & 0 & \frac{d_6}{3}B & \frac{d_6}{3}A \\ 0 & 0 & -d_6A & d_6B \\ -d_6B & \frac{d_6}{3}A & 2d_9B & -2d_9A \\ -d_6A & -\frac{d_6}{3}B & -2d_9A & -2d_9B \end{pmatrix}$$

produce first order approximations of the characteristic exponents of system (47). For the eigenvalues we find apart from the factor $7\varepsilon/2$:

$$\lambda^2 = -(A^2 + B^2) \left[\left(\frac{1}{3}d_6^2 - 2d_9^2 \right) \pm 2d_9 \sqrt{d_9^2 - \frac{1}{3}d_6^2} \right].$$

A sufficient condition for the complex case C to arise is

$$d_6^2 > 6d_9^2. \quad (48)$$

This condition corresponds with the condition in table 1 of [8]. Condition (48) is satisfied for $0 < u < u_1$ so that the complex case C arises for $u > 0$.

Another view of the eigenvalues is obtained by realizing that in subsection 4.1 we had $u = 0$ resulting in $d_6 \neq 0, d_9 = 0$; $u = 0$ gives for the x_2 normal mode purely imaginary eigenvalues with multiplicity two. As u increases ($d_9 \neq 0$), the eigenvalues move from the imaginary axis into the complex domain. This is part of the Hamiltonian-Hopf bifurcation, see fig. 7.

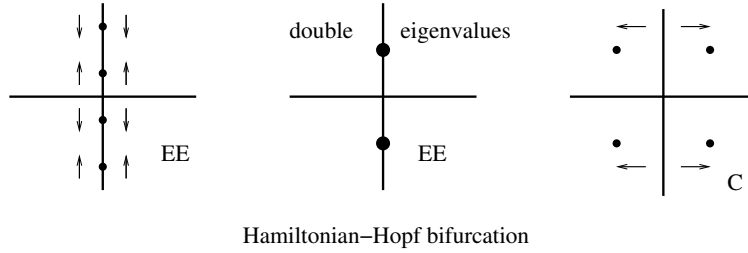


Figure 7: The Hamiltonian-Hopf bifurcation of a periodic solution in a three dof system as takes place for the x_2 normal mode in $1 : 2 : 3$ resonance of [8].

For case 2 (see subsection 4.3) we show in the action-simplex of fig. 8 the behaviour of solutions starting near this complex unstable normal mode.

The x_1 normal mode

For $d_9 = 0$ we have found in the preceding subsection the case HH. This is a generic case of eigenvalues, so for d_9 small enough the nature of the instability will not change but the dynamics is very different as the normal form is not integrable.

For case 2 (see subsection 4.3) we show in the action-simplex of fig. 9 the behaviour of solutions starting near this unstable normal mode.

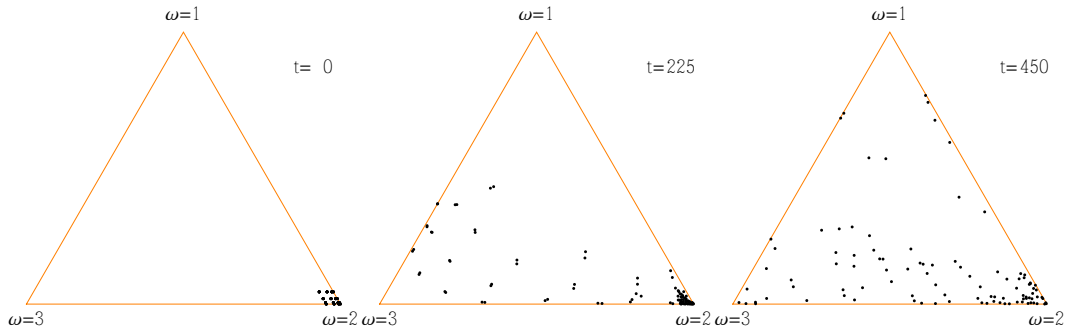


Figure 8: The $\omega = 2$ normal mode (x_2) exists in the case 2 and is complex unstable (see also fig. 6). We consider the time evolution of 98 initial positions near this normal mode by displaying the actions in the action-simplex at $t = 0, 225, 450$; $\varepsilon = 0.2$.

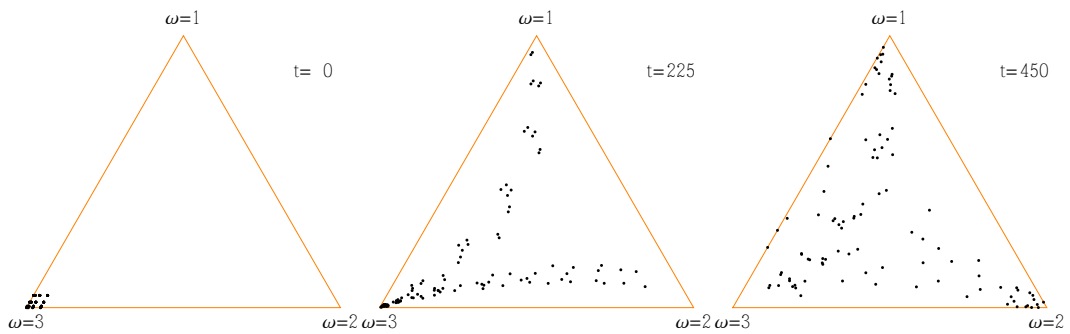


Figure 9: The $\omega = 3$ normal mode (x_1) exists in the case 2 and is unstable (see also fig. 6). We consider the time evolution of 98 initial positions near this normal mode by displaying the actions in the action-simplex at $t = 0, 225, 450$, $\varepsilon = 0.2$. The behaviour is different from the case 0, see fig. 4, as in this case the normal form is not integrable.

The periodic solution for $x_2(t) = 0$.

For the periodic solution (46) we put:

$$x_1 = C \cos 3t + D \sin 3t, \quad x_3 = A \cos t + B \sin t.$$

Transforming

$$x_1 = C \cos 3t + D \sin 3t + w_1, \quad x_2 = w_2, \quad x_3 = A \cos t + B \sin t + w_3,$$

and substitution into system (40), we find after linearization:

$$\begin{cases} \ddot{w}_1 + 9w_1 &= -\varepsilon 14d_6(A \cos t + B \sin t)w_2, \\ \ddot{w}_2 + 4w_2 &= -\varepsilon 14[d_6(C \cos 3t + D \sin 3t)w_1 + \\ & \quad d_6(A \cos t + B \sin t)w_1 + 2d_9(A \cos t + B \sin t)w_3], \\ \ddot{w}_3 + w_3 &= -\varepsilon 14[d_6(C \cos 3t + D \sin 3t)w_2 + 2d_9(A \cos t + B \sin t)w_2]. \end{cases} \quad (49)$$

To investigate stability we normalize near the periodic solution; apart from a factor $7\varepsilon/2$, this produces the matrix:

$$\begin{pmatrix} 0 & 0 & \frac{d_6}{3}B & \frac{d_6}{6}A & 0 & 0 \\ 0 & 0 & -d_6A & \frac{d_6}{2}B & 0 & 0 \\ -\frac{d_6}{2}B & \frac{d_6}{6}A & 0 & 0 & d_6\frac{D}{2} + d_9B & -d_6\frac{C}{2} + d_9A \\ -d_6A & -\frac{d_6}{3}B & 0 & 0 & -d_6C - 2d_9A & -d_6D + 2d_9B \\ 0 & 0 & d_6D - 2d_9B & -d_6\frac{C}{2} + d_9A & 0 & 0 \\ 0 & 0 & -d_6C - 2d_9A & -d_6\frac{D}{2} - d_9B & 0 & 0 \end{pmatrix}.$$

Using the values of C and D given in (46), we find purely imaginary eigenvalues with multiplicity two. The results have been summarized in fig. 6.

4.3 Experiments for two cases with $u > 0$

We consider a few experiments for two cases that are typical for the dynamics when $u > 0$.

Case 1 with less-balanced masses

We choose for $u = 0.534105$ from eqs. (17) and (18):

$$a_1 = 0.00510292, \quad a_2 = 0.117265, \quad a_3 = 0.0854008, \quad a_4 = 0.292231$$

In this case we have $m_1 > m_3 > m_2 > m_4$. With these mass (a_i) values the symplectic transformation of subsection 3.6 to system (39) produces the expression:

$$\begin{aligned} H_3 &= 0.0281999x_1^3 - 0.0258437x_1^2x_2 - 0.0777574x_1^2x_3 - 0.0275058x_1x_2^2 - 0.00252349x_1x_3^2 \\ &\quad - 0.0306229x_1x_2x_3 + 0.0157538x_2^3 + 0.000502655x_3^3 - 0.0089438x_2x_3^2 + 0.028527x_2^2x_3. \end{aligned}$$

We have the case:

$$d_6 = -0.0306229, \quad d_9 = -0.0089438.$$

so that the x_2 normal mode is complex unstable; see fig. 6. $H_2(t)$ time series are shown in figs. 10 and 11.

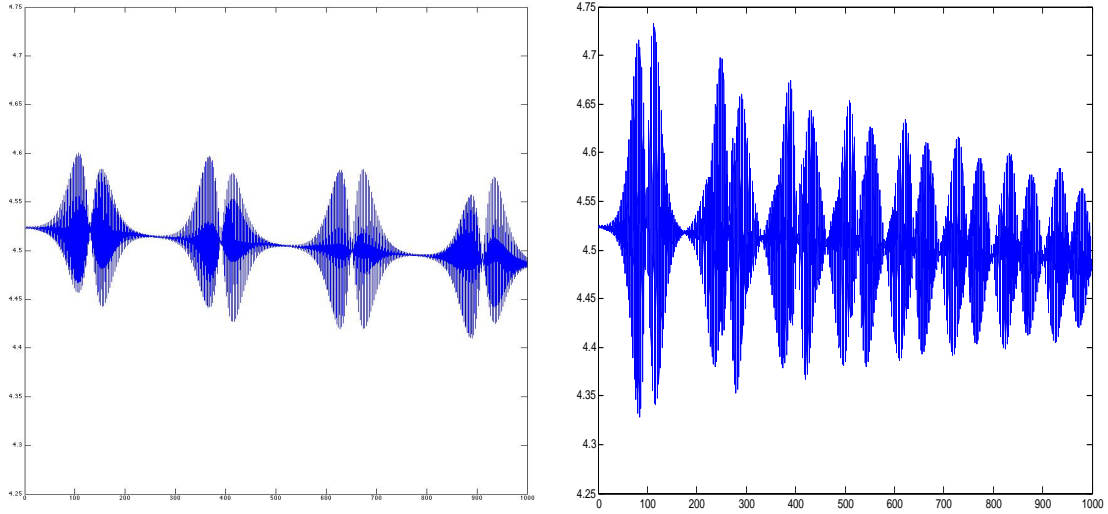


Figure 10: Left the $H_2(t)$ time series based on system (30), case 0, with initial values $x_1 = 1, x_2 = 0.1, x_3 = 0.1, \dot{x}_i = 0, i = 1, 2, 3; \varepsilon = 0.5, H_2(0) \approx 4.52$. Right the $H_2(t)$ time series for case 1 based on system (40) with the same initial conditions. Horizontal scales: time in $[0, 1000]$, vertical scales: energy in $[4.25, 4.75]$.

Note that d_9 is still fairly small with the implication that the expansion of the flow near the x_2 normal mode will not be very explosive. This may reduce the amount of chaos present in the system. We will compare with case 0 and give a few more details for different initial conditions based on integration of system (30) and system (40). We established that in all cases the x_1 normal mode is unstable (HH), see also fig. 6. Starting near the x_1 normal mode in case 0, the solutions move away, guided by the two-dimensional unstable manifold of the normal mode; the integrability of the normal form produces a fairly regular $H_2(t)$, see fig. 10. Also in this figure we display $H_2(t)$ for case 1 with the same initial conditions; its behaviour is influenced by the chaotic character of the normal form. On this interval of time $[0, 1000]$, energy is clearly pumped into H_3 but the recurrence of the Hamiltonian system will return this on a much longer timescale.

The chaos in case 1 (and 2) is strongly influenced by the complex instability of the x_2 normal mode. In case 0 this mode is stable so that $H_2(t)$ will vary even less. Using the same initial conditions for case 1 we find strong variations of $H_2(t)$, but always within the limits of the error estimates; see fig. 11.

Case 2 with less-balanced masses

We choose for $u = 0.826713$ from eqs. (17) and (18) a case with even less balanced masses; in this case m_1 is quite massive. We have:

$$a_1 = 0.000685158, a_2 = 0.11239, a_3 = 0.100269, a_4 = 0.286656.$$

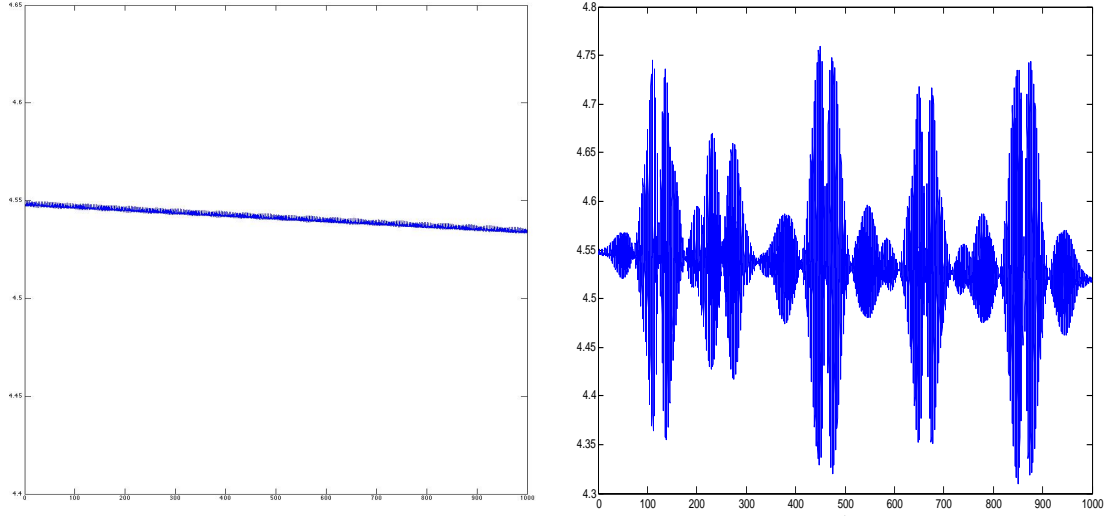


Figure 11: Left the $H_2(t)$ time series based on system (30), case 0, with initial values $x_1 = 0.1, x_2 = 1.5, x_3 = 0.1, \dot{x}_i = 0, i = 1, 2, 3; \varepsilon = 0.5, H_2(0) \approx 4.52$. Right the $H_2(t)$ time series for case 1 based on system (40) with the same initial conditions i.e. near the complex unstable x_2 normal mode. Horizontal scales: time in $[0, 1000]$, vertical scales: energy in $[4.4, 4.65]$ (left) and in $[4.3, 4.8]$ (right).

With these mass (a_i) values the symplectic transformation of subsection 3.6 to system (39) produces the expression:

$$H_3 = 0.0352657x_1^3 - 0.0272316x_1^2x_2 - 0.0743155x_1^2x_3 - 0.0366184x_1x_2^2 - 0.00260064x_1x_3^2 - 0.0337877x_1x_2x_3 + 0.0181144x_2^3 + 0.000760425x_3^3 - 0.0105601x_2x_3^2 + 0.023904x_2^2x_3.$$

We have the case:

$$d_6 = -0.0337877, d_9 = -0.0105601$$

If $d_9 \neq 0$ (the cases 1 and 2), the x_3 normal mode does not exist. In fig. 12 we show the action-simplex for solutions starting near the $x_1 = x_2 = 0$ position, so near the $\omega = 1$ vertex.

We present the $H_2(t)$ time series based on system (40) in fig. 13.

4.4 Comparison with another Hamiltonian system in 1 : 2 : 3 resonance

We will discuss our results for the inhomogeneous FPU chain with another Hamiltonian system in 1 : 2 : 3 resonance, and compare the instability types of the x_2 normal mode.

For the inhomogeneous FPU lattice in 1 : 2 : 3 resonance we found complex instability (C) of the x_2 normal mode and no cases of HH instability. Both cases, HH and C lead to a non-integrable normal form but the dynamics is different. See [2].

To illustrate the different dynamics consider the Hamiltonian presented as an example in [18]:

$$H(p, q) = \frac{1}{2}(p_1^2 + q_1^2) + (p_2^2 + q_2^2) + \frac{3}{2}(p_3^2 + q_3^2) - \varepsilon q_1^2(a_2q_2 + a_3q_3) - \varepsilon b q_1 q_2 q_3. \quad (50)$$

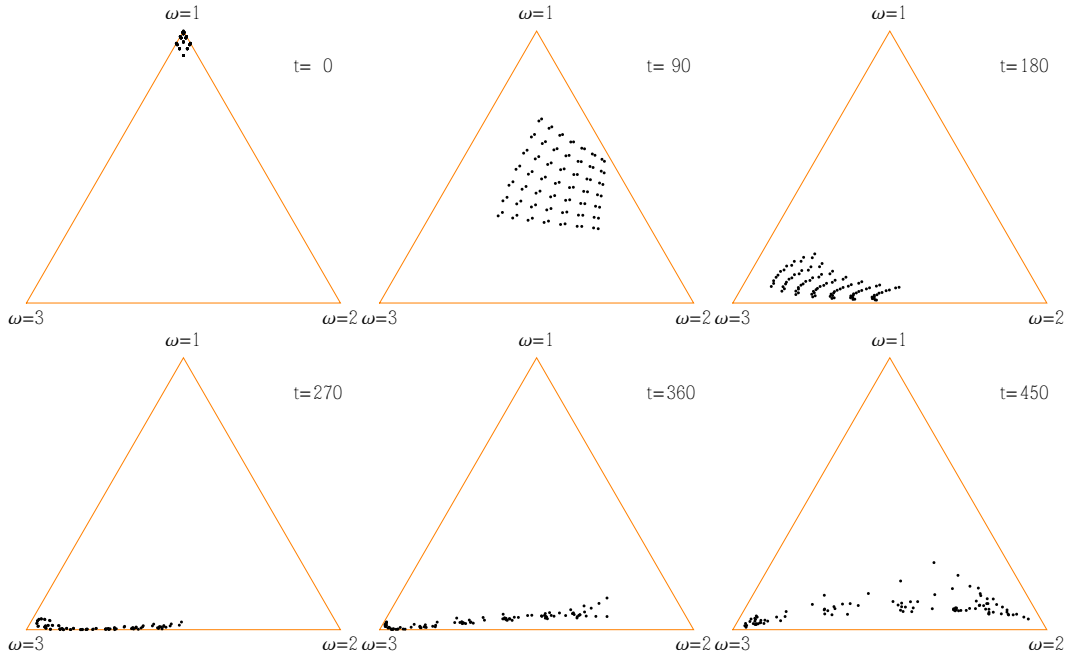


Figure 12: We consider for case 2 the time evolution of 98 starting points near the $\omega = 1$ vertex by displaying the action-simplex at various times.

This system is in $1 : 2 : 3$ resonance but it is not derived from a FPU chain. We present $H_2(t)$ for both cases in fig. 14. The dynamics is chaotic but in the case left, the q_2 normal mode is unstable with real eigenvalues (HH); transverse homoclinic intersections produce chaotic motion. On the right the q_2 normal mode is complex unstable (C) which produces the Hamiltonian Devaney-Shilnikov phenomenon. This involves a homoclinic orbit surrounded by an infinite number of unstable periodic solutions producing more violent chaotic motion as predicted in [3].

5 Conclusions

General

- For an inhomogeneous periodic FPU-chain with four particles, most frequency ratios occur for a one-dimensional variety of mass ratios. The frequency ratios $1 : 2 : 1$ and $1 : 1 : 3$ arise for a finite number of mass ratios, the ratios $1 : 2 : 2$, $1 : 1 : 1$ and $1 : 3 : 3$ do not occur at all in this FPU-chain. See table 1.
- For any number of particles $n \geq 3$ the set of mass distributions for a given frequency distribution has a relatively simple algebraic structure. For $n = 4$ we describe algorithmically how to determine this set for a given frequency distribution. For $n \geq 4$ there are frequency distributions that do not correspond to any mass distribution.

The case of four particles in $1 : 2 : 3$ resonance

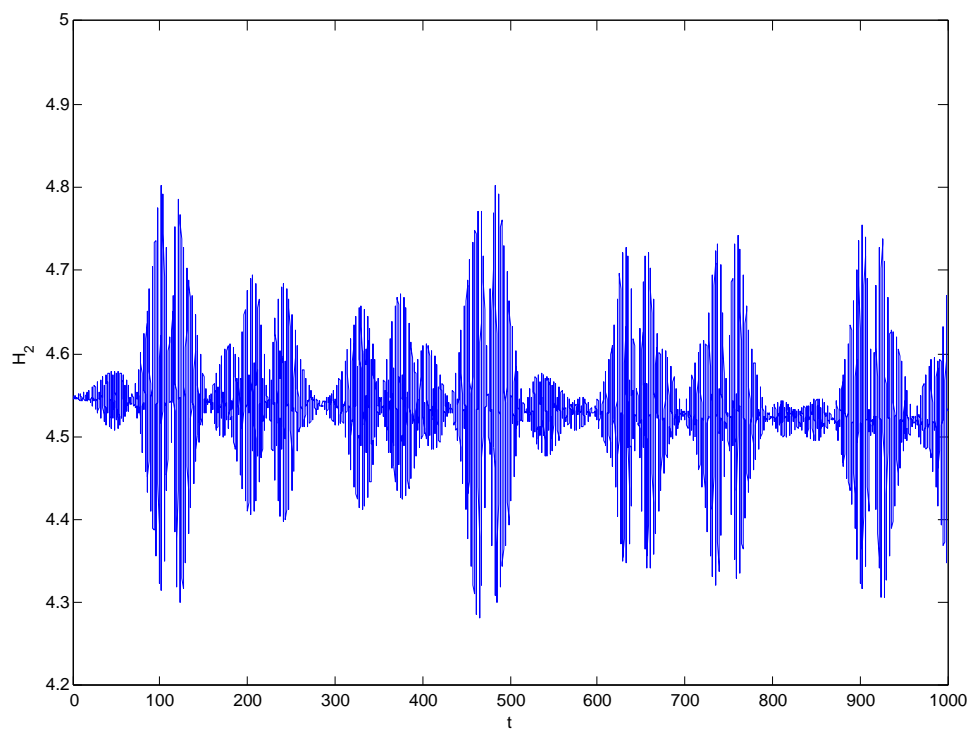


Figure 13: The $H_2(t)$ -time series 0 – 1000 based on system (40), case 2, with initial values $x_1 = 0.1, x_2 = 1.5, x_3 = 0.1, \dot{x}_1 = \dot{x}_2 = \dot{x}_3 = 0, \varepsilon = 0.5$.

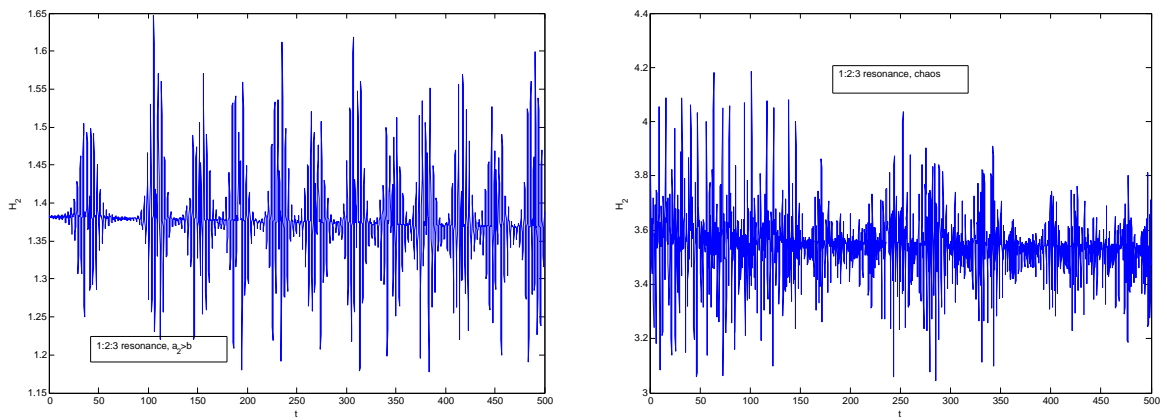


Figure 14: Two $H_2(t)$ time series based on Hamiltonian (50). On the left $x_1(0) = 0.1$, $x_2(0) = 1$, $x_3(0) = 0.5$, and on the right $x_1(0) = 2$, $x_2(0) = 1$, $x_3(0) = -0.05$. For both time series we use $\varepsilon = 0.5$, $a_2 = 3$, $a_3 = 1$, $b = 1$, and $\dot{x}_1(0) = \dot{x}_2(0) = \dot{x}_3(0) = 0$.

For the x_2 normal mode we have instability HH on the left and instability C on the right. In both cases the Hamiltonian flow is chaotic but in the right picture the system has undergone Devaney-Shilnikov bifurcation.

Horizontal scales: time in $[0, 500]$, vertical scales: energy in $[1.15, 1.65]$ (left) and in $[3, 4.5]$ (right).

- A special case of the resonance $1 : 2 : 3$ has the symmetry of two equal masses and two quite different masses. Along the variety of mass ratios as a limit case one of the masses tends to infinity.
- The symmetric case of two equal masses differs dynamically from the other cases. The transition corresponds to a Hamiltonian-Hopf bifurcation with a Shilnikov-Devaney bifurcation producing chaotic dynamics. In a more general context such behaviour of the $1 : 2 : 3$ resonance was described in [8].
- The normalized system for the symmetric case of two equal masses is integrable and has periodic solutions for each of the three eigenmodes (the normal modes). Moreover, there are on the energy manifold two families of periodic solutions connecting the second and the third eigenmode. This is a degeneration in the sense described by Poincaré [10], vol. 1.
- Under the transition away from the symmetric case, the eigenmodes x_1 (associated with frequency 3) and x_2 (associated with frequency 2) produce a periodic solution (normal mode) in the nonlinear system. The periodic solution that was associated to the third eigenmode in the symmetric case moves away along an edge of the action simplex. The two continuous families of periodic solutions of the symmetric case break up into four periodic solutions.
- The inhomogeneous periodic FPU α -chain with four particles is characterized by a non-integrable normal form, except in the symmetric case of two equal masses. The implication is that near stable equilibrium its chaotic behaviour is not restricted to exponentially small sets as in the case of two dof systems and as in the case of the classical FPU α -chain. In this sense the model of the classical FPU-chain is misleading.

A Further details for the spectrum induced by H_2

Here we give a further discussion of results mentioned in section 3.

A.1 Fiber contained in a quadratic set

For given eigenvalues $\lambda_1 \geq \lambda_2 \geq \dots \geq \lambda_{n-1} > \lambda_n = 0$ of $A_n C_n$ (see subsection 3.1) we have the relations (7) for the elements (a_1, \dots, a_n) in the corresponding fiber. Here we will use the last two relations, given in (8).

Lemma A.1

The polynomials p_{n-1} and p_{n-2} have the form indicated in (8).

Proof. If we replace the entries -1 at positions $(1, n)$ and $(n, 1)$ in C_n by 0 we obtain the Cartan matrix \mathcal{C}_n for the root system of type A_n . (See, eg., [1, Déf. 3 in 1.5 of Chap. 6, and Planche I].) The determinant of \mathcal{C}_n is known to be $n + 1$.

If all a_j are non-zero, the characteristic equation is equivalent to $\det(C_n - \lambda A^{-1}) = 0$. We determine first the factor of $(-\lambda)^{n-1}$. In the expansion of the determinant the term with λ at all diagonal positions except at (j, j) is equal to

$$2 \prod_{i \neq j} (-\lambda a_i^{-1}) = 2(-\lambda)^{n-1} a_j / (a_1 a_2 \cdots a_n).$$

So the factor of $(-\lambda)^{n-1}$ in $\det(AC_n - \lambda I_n)$ is $\sum_j 2a_j = p_{n-1}(a)$.

For the factor of $(-\lambda)^{n-2}$ we have contributions of two types: Two diagonal positions j and $j+1$ (modulo n) lead to a contribution of the form $\det(\mathcal{C}_2) \prod_{i \neq j, j+1} (-\lambda)/a_i$. Two non-adjointing diagonal positions j_1, j_2 contribute $2 \cdot 2 \sum_{i \neq j_1, j_2} (-\lambda)/a_i$. This leads to the description of $p_{n-2}(a)$. \square

By scaling we arrange that the vectors $(\lambda_1, \dots, \lambda_{n-1}, 0)$ of eigenvalues of $A_n C_n$ satisfy $\sum_{j=1}^{n-1} \lambda_j = 1$, and we put $\eta = e_2(\lambda_1, \dots, \lambda_{n-1})$. Then the points of the fiber of a given vector of eigenvalues are elements of the following set Q_η :

Proposition A.2

Let $n \geq 3$. For given $\eta > 0$ denote by Q_η the set of points $a \in \mathbb{R}^n$ satisfying

$$p_{n-2}(a) = \eta, \quad p_{n-1}(a) = \frac{1}{2}. \quad (51)$$

Then

- a) If $\eta < \frac{1}{2} - \frac{3}{4n}$, then Q_η is a compact quadric in the hyperplane $a_1 + \dots + a_n = \frac{1}{2}$ in \mathbb{R}^n with a non-empty intersection with $\mathbb{R}_{>0}^n$.
- b) If $\eta = \frac{1}{2} - \frac{3}{4n}$, then Q_η consists of one point in $\mathbb{R}_{>0}^n$.
- c) If $\eta > \frac{1}{2} - \frac{3}{4n}$, then $Q_\eta = \emptyset$.

Proof. Let $P = C_n - 6I_n + 4E$, with E the $n \times n$ -matrix with all elements equal to 1. Then, considering $a = (a_1, \dots, a_n)$ as a row vector, we have

$$q_{n-2}(a) = \frac{1}{2} a P a^T.$$

To see this we check that P is the matrix

$$\begin{pmatrix} 0 & 3 & 4 & \cdots & 4 & 3 \\ 3 & 0 & 3 & \cdots & 4 & 4 \\ 4 & 3 & 0 & \cdots & 4 & 4 \\ \vdots & \vdots & \vdots & \ddots & \vdots & \vdots \\ 4 & 4 & 4 & \cdots & 0 & 3 \\ 3 & 4 & 4 & \cdots & 3 & 0 \end{pmatrix}$$

There are orthogonal matrices U such that $U^T C_n U = \Lambda$, where Λ is the diagonal matrix with the eigenvalues λ_j of C_n on the diagonal. We put the eigenvalue 0, with eigenvector \mathbf{e} as the last one. Then $\mathbf{e} = (0, \dots, 0, \sqrt{n})U^T$. This gives

$$p_{n-1}(a) = 2 \sum_j a_j = 2a\mathbf{e}^T = 2\sqrt{n}(aU)_n,$$

$$p_{n-2}(a) = \frac{1}{2} a(C_n - 6I_n)a^T + 2aEa^T = \frac{1}{2} aU(\Lambda - 6I_n)U^T a^T + \frac{1}{2} (p_{n-1}(a))^2.$$

The points in the hyperplane $p_{n-1}(a) = 1$ can be described as

$$a = \left(x_1, x_2, \dots, x_{n-1}, \frac{1}{2\sqrt{n}} \right) U^T.$$

We write $x = (x_1, \dots, x_{n-1})^T$. We find the equation

$$\begin{aligned} \eta &= \frac{1}{2}(x, 1/(2\sqrt{n}))(\Lambda - 6I)(x, 1/(2\sqrt{n}))^T + \frac{1}{2} \\ &= -\sum_{j=1}^{n-1} \frac{6 - \lambda_j}{2} x_j^2 + \frac{1}{2} - \frac{3}{4n}. \end{aligned} \quad (52)$$

So the points run through a quadratic set in the hyperplane $p_{n-1}(a) = 1$. The eigenvectors of C_n can be chosen as $(\zeta^k, \zeta^{2k}, \dots, \zeta^{nk})$ with $\zeta = e^{2\pi i/n}$, which leads to eigenvalues $2 - 2\cos 2\pi k/n \in [0, 4]$. So the $\lambda_j - 6$ are strictly negative. The equation becomes

$$\sum_{j=1}^{n-1} \frac{6 - \lambda_j}{2} x_j^2 = \frac{1}{2} - \frac{3}{4n} - \eta. \quad (53)$$

In case b) in the proposition the single point $x = 0$ corresponds to $\frac{1}{2n}\mathbf{e} \in \mathbb{R}_{>0}^n$. As η decreases the quadric expands in all directions, some of these stay inside $\mathbb{R}_{>0}^n$. \square

Corollary A.3

If $n = 3$ each choice of eigenvalues $\lambda_1 \geq \lambda_2 > \lambda_3 = 0$ of A_3C_3 occurs for some positive diagonal matrix A_3 .

If $n \geq 4$, there are choices of eigenvalues $\lambda_1 \geq \lambda_2 \geq \dots \geq \lambda_{n-1} > \lambda_n = 0$ for which there are no positive diagonal matrices A_n such that A_nC_n has these eigenvalues.

Proof. The choice $\lambda_1 = \dots = \lambda_{n-1} = \frac{1}{n-1}$ leads to

$$\eta = e_2(\{\lambda_1, \dots, \lambda_{n-1}\}) = \binom{n-1}{2} / (n-1)^2 = \frac{1}{2} - \frac{1}{2(n-1)}.$$

This is at most $\frac{1}{2} - \frac{3}{4n}$ if $n = 3$. This establishes the second assertion.

For $n = 3$ we have $\lambda_1 + \lambda_2 = 1$, hence $\eta = \lambda_1\lambda_2 \leq \frac{1}{4} = \frac{1}{2} - \frac{3}{4 \cdot 3}$. \square

A.1.1 Spherical coordinates.

In the case $n = 4$ we may take the orthogonal matrix in the proof of the proposition in the form

$$U = \begin{pmatrix} -\frac{1}{2} & 0 & \frac{-1}{\sqrt{2}} & \frac{1}{2} \\ \frac{1}{2} & \frac{-1}{\sqrt{2}} & 0 & \frac{1}{2} \\ -\frac{1}{2} & 0 & \frac{1}{\sqrt{2}} & \frac{1}{2} \\ \frac{1}{2} & \frac{1}{\sqrt{2}} & 0 & \frac{1}{2} \end{pmatrix},$$

corresponding to the eigenvalues 4, 2, 2, 0. This gives

$$\begin{aligned} x_1 &= \frac{-a_1 + a_2 - a_3 + a_4}{2}, & x_2 &= \frac{a_4 - a_2}{\sqrt{2}}, \\ x_3 &= \frac{a_3 - a_1}{\sqrt{2}} \end{aligned} \quad (54)$$

Points of the fiber give points on the ellipsoid $x_1^2 + 2x_2^2 + 2x_3^2 = \frac{5}{16} - \eta$. Then spherical coordinates ψ and ϕ are determined by

$$\begin{aligned} x_1 &= \rho \sin \psi, & x_2 &= \frac{\rho}{\sqrt{2}} \cos \psi \cos \phi, & x_3 &= \frac{\rho}{\sqrt{2}} \cos \psi \sin \phi, \\ \rho &= \sqrt{\frac{5}{16} - \eta} > 0, & -\frac{\pi}{2} &\leq \psi \leq \frac{\pi}{2}, & -\pi &\leq \phi \leq \pi. \end{aligned} \quad (55)$$

These are the spherical coordinates used in fig. 3.

A.2 Conditions for the fibers to be non-empty

For $n = 4$ the equations (9) determine whether points of the fibers exist. In particular, a (scaled) choice of eigenvalues determines $\xi, \eta > 0$ which determine the equations for the fiber. We first consider the values of (ξ, η) that can occur:

Proposition A.4

Let $n = 4$. The set of $(\xi, \eta) = (e_3(\{\lambda_1, \lambda_2, \lambda_3\}), e_2(\{\lambda_1, \lambda_2, \lambda_3\}))$ where $(\lambda_1, \lambda_2, \lambda_3)$ runs through the open triangle in $\mathbb{R}_{>0}^3$ given by $\lambda_1 + \lambda_2 + \lambda_3 = 1$, satisfy

$$0 < \xi \leq \frac{1}{27}, \quad 0 < \eta \leq \frac{1}{3}, \quad T(\xi, \eta) \leq 0, \quad (56)$$

where

$$T(\xi, \eta) = 27\xi^2 + 4\eta^3 - 18\xi\eta - \eta^2 + 4\xi. \quad (57)$$

Illustration in fig. 15.

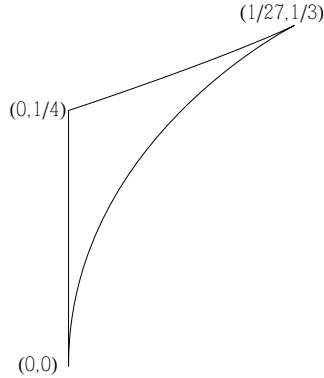


Figure 15: Region in the ξ - η -plane corresponding to choices of positive eigenvalues. (Horizontal axis: ξ ; vertical axis: η .)

Proof. We have to determine the image X of the triangle $T = \{(\lambda_1, \lambda_2, \lambda_3) \in \mathbb{R}_{>0} : \lambda_1 + \lambda_2 + \lambda_3 = 1\}$ under the map

$$\Phi : (\lambda_1, \lambda_2, \lambda_3) \mapsto (\xi, \eta) = (\lambda_1\lambda_2\lambda_3, \lambda_1\lambda_2 + \lambda_2\lambda_3 + \lambda_3\lambda_1).$$

If a point $(\lambda_1, \lambda_2, \lambda_3) \in T$ is mapped to the boundary of the image X , then the gradient of Φ has rank less than 2 at that point. That occurs if two of the coordinates are equal. By

S_3 -symmetry it suffices to consider $\lambda_2 = \lambda_3$. The image of the open segment $\{(1 - 2y, y, y) : 0 < y < \frac{1}{2}\}$ consists of the points

$$(\xi, \eta) = (y^2(1 - 2y), y(2 - 3y)).$$

These are points of the curve $T(\xi, \eta) = 0$. They run from $(0, 0)$ to the cusp at $(\frac{1}{27}, \frac{1}{3})$ and then to $(0, \frac{1}{4})$.

The boundary of T consists of three segments, one of them $\{(0, x, 1 - x) : 0 \leq x \leq 1\}$. The image is $\{(0, x(1 - x)) : 0 \leq x \leq 1\}$, the segment from $(\xi, \eta) = (0, 0)$ to $(0, \frac{1}{4})$. By S_3 -invariance the two other boundary segments have the same image.

The image X is the region enclosed by these boundary curves. \square

The points (ξ, η) for which the fiber is non-empty form a subset of the region in Proposition A.4. Corollary A.3 tells us that the fiber is empty for $(\frac{1}{27}, \frac{1}{3})$. We give a description of the set of (ξ, η) corresponding to non-empty fibers. A proof can be given along the same lines as that of Proposition A.4, but takes much more work. In the determination of the fibers according to the computational scheme in the next subsection it becomes clear anyhow whether the fiber is empty or not.

Proposition A.5

The set of points (ξ, η) corresponding to a non-empty fiber is equal to

$$\left\{ (\xi, \eta) \in \mathbb{R}_{>0}^2 : 0 < \xi \leq \frac{1}{32}, 0 < \eta \leq 2\xi + \frac{1}{4}, T(\xi, \eta) \leq 0 \right\}, \quad (58)$$

with T as defined in (57).

The points (ξ, η) for which the fiber is not compact constitute the subset

$$\left\{ (\xi, \eta) \in (0, \frac{1}{32}) \times (0, \frac{5}{16}) : 8\xi^2 + \eta^3 - 5\xi\eta - \frac{1}{4}\eta^2 + \frac{9}{8}\xi \leq 0 \right\}. \quad (59)$$

Illustrations in fig. 16.

A.3 Computation of fibers

The computation carried out in subsection 3.4 for the resonance $(1 : 2 : 3)$ is guided by the use of the action of the dihedral group D_4 on the solutions. We start with the quantities $\xi, \eta, \eta_1, \eta_2$, which are invariant under the whole group D_4 .

In the next stage we consider the quantity $4(-a_1 + a_2 - a_3 + a_4) = \sqrt{1 - 16\eta_2}$ which is invariant under the subgroup $V_4 \subset D_4$ generated by the permutations $[1, 3]$ and $[2, 4]$. This quantity is sent to its negative by $[1, 2][3, 4]$. The group V_4 also leaves invariant $s_{13}, s_{24}, p_{13}, p_{24}$. (If $\eta = 4\xi + \frac{3}{16}$ then we can take $\eta_2 = \frac{1}{16}$. In that situation p_{13} and p_{24} are not uniquely determined.)

In the next stage we determine a_1 and a_3 , invariant under $[2, 4]$ and exchanged by $[1, 3]$. Similarly a_2 and a_4 are invariant under $[1, 3]$ and exchanged by $[2, 4]$. The total solution (a_1, a_2, a_3, a_4) is changed by non-trivial elements of D_4 , except in cases with additional symmetry.

In Table 3 the resulting computational scheme is described. It works under the assumption that the point (ξ, η) is not on the line $\eta = 4\xi + \frac{3}{16}$, illustrated in fig. 17. The parameter u

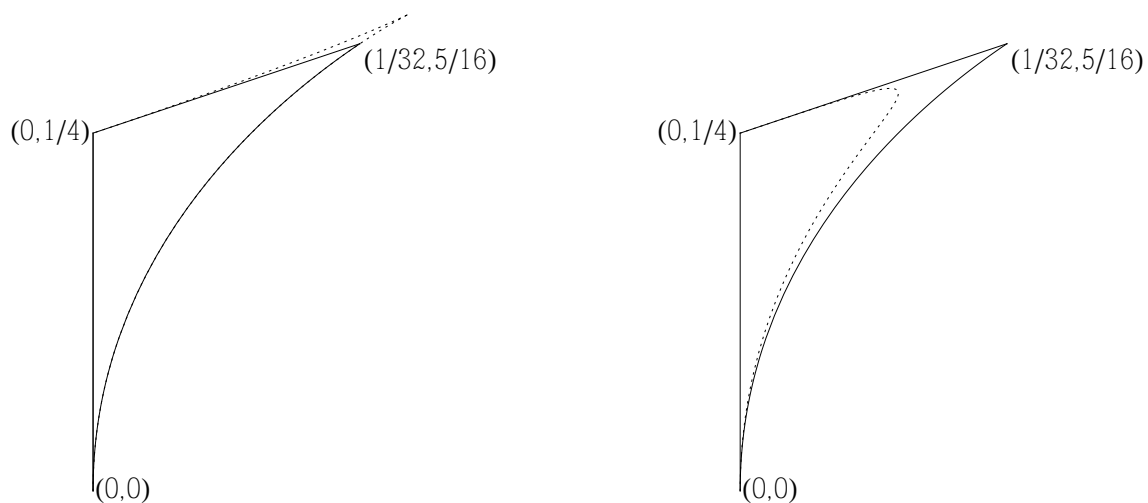


Figure 16: On the left the region in (58) of points (ζ, η) corresponding to non-empty fibers. The dotted line gives (part of) the boundary of the larger region in Proposition A.4, corresponding to choices of positive eigenvalues. This shows that most of the possible combinations (ζ, η) correspond to a non-empty fiber. On the right is again the region in (58), with the subregion in (59) indicated by the dotted line. The points strictly to the right of the dotted line correspond to compact fibers.

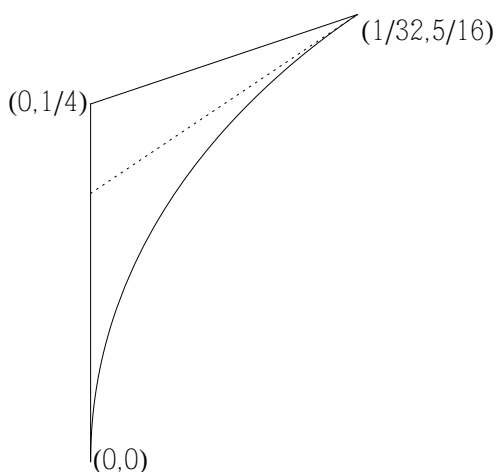


Figure 17: The points on the dotted line $\eta = 4\zeta + \frac{3}{16}$ between $(0, \frac{3}{16})$ and $(\frac{1}{32}, \frac{5}{16})$ correspond to fibers for which the computational scheme in Table 3 is incomplete. None of the resonances in Table 1 correspond to points on this exceptional line.

i. For given positive eigenvalues put

$$\eta = \frac{\lambda_1\lambda_2 + \lambda_2\lambda_3 + \lambda_3\lambda_1}{(\lambda_1 + \lambda_2 + \lambda_3)^2}, \quad \zeta = \frac{\lambda_1\lambda_2\lambda_3}{(\lambda_1 + \lambda_2 + \lambda_3)^3}.$$

ii. Write $\eta = 4\eta_1 + 3\eta_2$. Determine the subinterval $I_1 \subset (0, \frac{1}{16})$ such that $\eta_1 > 0$ for $\eta_2 \in I_1$.

iii. Compute

$$s_{13} = \frac{1 - \sqrt{1 - 16\eta_2}}{4}, \quad s_{24} = \frac{1 + \sqrt{1 - 16\eta_2}}{4},$$

$$p_{13} = \frac{\zeta/4 - s_{13}\eta_1}{\sqrt{1 - 16\eta_2}/2}, \quad p_{24} = \eta_1 - p_{13}.$$

Determine the subset $I_2 \subset I_1$ such that $p_{13} > 0$ and $p_{24} > 0$ for $\eta_2 \in I_2$.

iv. Compute $d_{13} = s_{13}^2 - 4p_{13}$ and $d_{24} = s_{24}^2 - 4p_{24}^2$. Determine $I_3 \subset I_2$ such that $d_{13} \geq 0$ and $d_{24} \geq 0$.

v. Compute $a_1, a_3 = \frac{1}{2}(s_{13} \mp \sqrt{d_{13}})$ and $a_2, a_4 = \frac{1}{2}(s_{24} \mp \sqrt{d_{24}})$. Determine the subset $I_4 \subset I_3$ such that $a_j > 0$ for $j = 1, \dots, 4$ for $\eta_2 \in I_4$.

vi. Apply all symmetries in the dihedral group D_4 to the points (a_1, \dots, a_4) .

Table 3: Instructions to compute fibers for the case $n = 4$. In these instructions we assume that $\eta \neq 4\zeta + \frac{3}{16}$. Otherwise we also have to consider $p_{13} \in (0, \zeta)$ and investigate whether this leads to further solutions.

was specially adapted to the resonance $(1 : 2 : 3)$. Here we use $\eta_2 \in (0, \frac{1}{16})$ as the parameter.

We apply the computational scheme to the resonances $(1 : 2 : 2)$, $(1 : 1 : 2)$, $(1 : 3 : 6)$ and $(2 : 3 : 4)$. Together with the resonance $(1 : 2 : 3)$ considered in subsection 3.4 these are representative examples of the cases in Table 1.

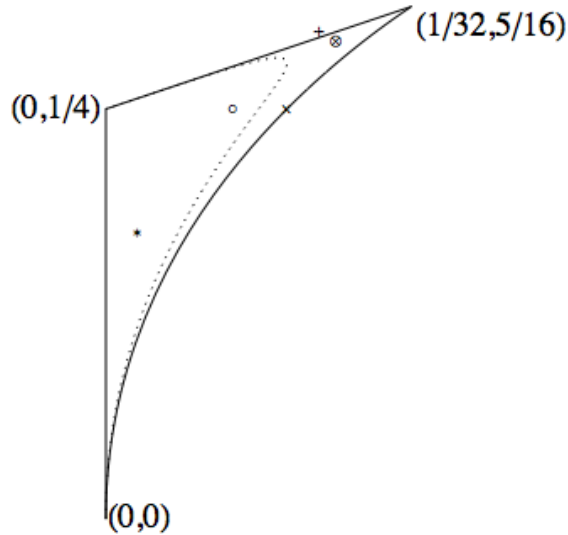


Figure 18: Points corresponding to the resonances $(1 : 2 : 3)$ (\circ), $(1 : 2 : 2)$ ($+$), $(1 : 1 : 2)$ (\times), $(1 : 3 : 6)$ ($*$), and $(2 : 3 : 4)$ (\otimes).

A.3.1 Resonance $(1 : 2 : 2)$

To $(\lambda_1, \lambda_2, \lambda_3) = (\frac{4}{9}, \frac{4}{9}, \frac{1}{9})$ corresponds $(\xi, \eta) = (\frac{16}{729}, \frac{8}{27})$. In fig. 18 it is hard to see whether it is in the region described in (58). A direct computation shows that $\eta > 2\xi + \frac{1}{4}$, so the fiber is empty.

If we carry out the steps in the computational scheme, the set of values that η_2 may have becomes empty when we check whether $d_{24} \geq 0$.

A.3.2 Resonance $(1 : 1 : 2)$

With $(\lambda_1, \lambda_2, \lambda_3) = (\frac{2}{3}, \frac{1}{6}, \frac{1}{6})$ we have $(\xi, \eta) = (\frac{1}{54}, \frac{1}{4})$. The corresponding point seems to be on the boundary of the region for a non-empty fiber. It turns out that $T(\xi, \eta)$ is exactly 0.

Following the computational scheme the expression for d_{13} in terms of η_2 turns out to be non-positive for $\eta_1 \in (0, \frac{1}{16})$, with a zero only at $\eta_2 = \frac{1}{18}$. This leads to the solution

$$(a_1, \dots, a_4) = \left(\frac{1}{12}, \frac{2 - \sqrt{2}}{12}, \frac{1}{12}, \frac{2 + \sqrt{2}}{12} \right). \quad (60)$$

It is invariant under the substitution (13) in the dihedral group. See fig. 19.

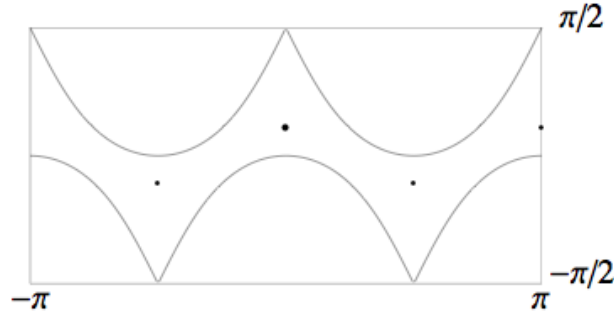


Figure 19: The fiber for the resonance (1 : 1 : 2) (subsection A.3.2) in spherical coordinates as described in subsection A.1.1. The thick point corresponds to the vector in (60), the other points are its translates under elements of D_4 . The curved line indicates the boundary of the region with positive coordinates.

A.3.3 Resonance (1 : 3 : 6)

For $(\lambda_1, \lambda_2, \lambda_3) = (\frac{18}{23}, \frac{9}{46}, \frac{1}{46})$ we have $(\xi, \eta) = (\frac{81}{24334}, \frac{369}{2116})$. The corresponding point in fig. 18 is to the left of the dotted line. This indicates that the fiber contains open curves.

The computational scheme gives solutions for

$$\eta_2 \in \left[\frac{11}{1058}, h_2 \right) \cup (h_3, h_4),$$

with algebraic numbers $h_2 \approx .112814$, $h_3 \approx .0501346$, $h_4 \approx .0548411$. For $\eta_2 = \frac{11}{1058}$ we find a point that is invariant under $(13) \in D_4$. Fig. 20 illustrates the fiber.

A.3.4 Resonance (2 : 3 : 4)

For $(\lambda_1, \lambda_2, \lambda_3) = (\frac{16}{29}, \frac{9}{19}, \frac{4}{29})$ we have $(\xi, \eta) = (\frac{576}{24389}, \frac{244}{841})$. The corresponding point in fig. (18) is in the region where the fiber is compact. With the relations in subsection A.1.1 one can check that all a_j are positive on the ellipsoid for $\eta = \frac{244}{841}$.

The computational schema gives a family of solutions depending on $\eta_2 \in [\frac{42}{841}, \frac{99}{1682}]$. The end points give symmetric solutions: $a_1 = a_3$ for $\eta_2 = \frac{42}{841}$, and $a_2 = a_4$ for $\eta_2 = \frac{99}{1682}$. In fig. 21 we see that the fiber consists of two closed curves.

A.4 Transformation matrices for the resonance (1 : 2 : 3)

In subsection 3.4 we computed functions $u \mapsto a_j(u)$, $1 \leq j \leq 4$, on the interval $[0, u_1)$ as diagonal elements of a diagonal matrix $A_4(u)$ such that $A_4(u) C_4$ has eigenvalues $\frac{9}{14}, \frac{4}{14}, \frac{1}{14}, 0$. For the transformation to eigenmodes of the Hamiltonian we need in subsection 3.6 a family of orthogonal matrices $u \mapsto U(u)$ such that $U(u)$ diagonalizes $A_4(u)^{1/2} C_4 A_4(u)^{1/2}$. For any value of u such orthogonal matrices can be found numerically. Here we want to describe explicitly the dependence on $u \in [0, u_1)$. The version 9.0.1.0 of MATHEMATICA that we used had difficulties with the symbolic computations. Hence we indicate how we proceeded.

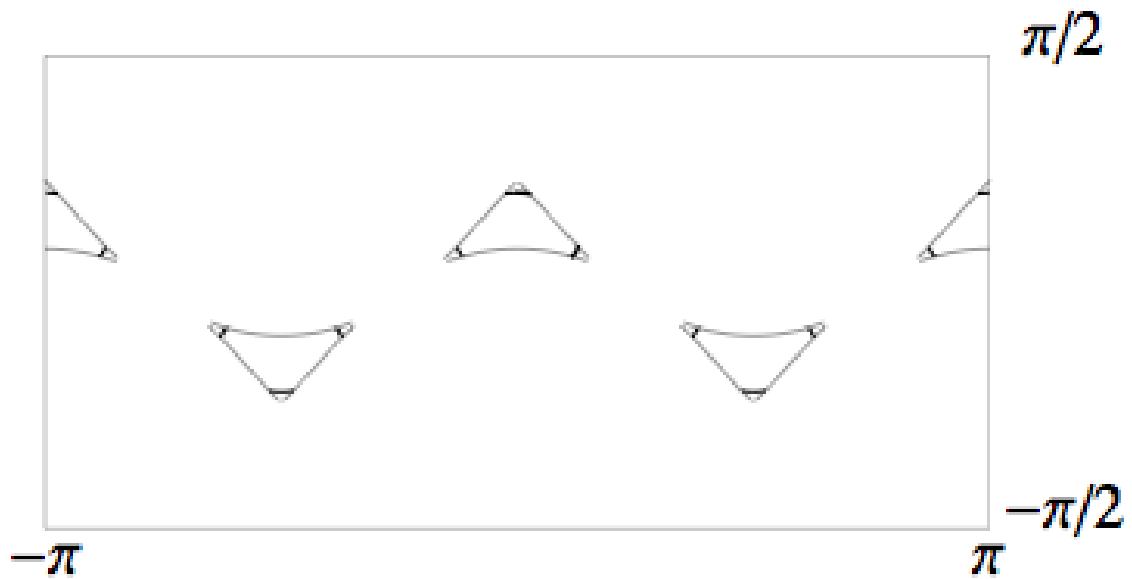


Figure 20: The fiber for the resonance $(1 : 3 : 6)$ in spherical coordinates, as described in subsection A.1.1.

The interior of the four triangles correspond to the region with positive coordinates. The fiber consists of twelve open curves, three in each triangle. The curves obtained with the computational scheme are drawn thicker than their translates under the dihedral group.

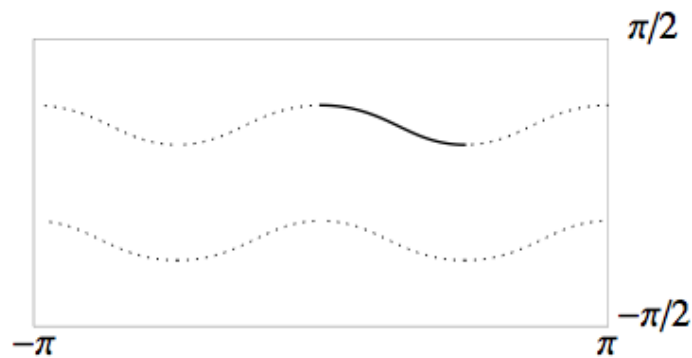


Figure 21: The fiber for the resonance $(2 : 3 : 4)$ in spherical coordinates, as described in subsection A.1.1.

The thick line corresponds to the solutions obtained by the computational scheme. The dotted lines are formed by the translates under D_4 of the computed part. In this case all points on the ellipsoid have positive coordinates.

Lemma A.6

Let A_4 be a positive diagonal matrix with diagonal elements a_1, \dots, a_4 . Let λ be an eigenvalue of $A_4 C_4$ such that $\lambda \neq 2a_j$ for $1 \leq j \leq 4$. Put

$$\mu_j = \frac{1}{2 - \lambda/a_j}.$$

Then

$$(\mu_1(\mu_2 + \mu_4), \mu_2, \mu_3(\mu_2 + \mu_4), \mu_4)$$

is an eigenvector of $A_4 C_4$ for the eigenvalue λ .

Proof. We have

$$C_4 - \lambda A^{-1} = \begin{pmatrix} \mu_1^{-1} & -1 & 0 & -1 \\ -1 & \mu_2^{-1} & -1 & 0 \\ 0 & -1 & \mu_3^{-1} & -1 \\ -1 & 0 & -1 & \mu_4^{-1} \end{pmatrix}.$$

We try to solve $(C - \lambda A^{-1})v = 0$ with $v = (p, x, q, y)$. The first and third lines give $x + y = \mu_1^{-1}p = \mu_3^{-1}q$. Similarly, we get $p + q = \mu_2^{-1}x = \mu_4^{-1}y$. Since λ is an eigenvalue of $A_4 C_4$ there are non-zero solutions, for which x and y both have to be non-zero. So there is a solution with $x = \mu_2$. Then we obtain the vector in the lemma. \square

Now we take for a_j the expressions in (17) and (18). It is clear that $2a_j(u) - \lambda_i$ is not identically zero in u for any of the four eigenvalues λ_i and any j . So we obtain vectors $v_i(u)$, $1 \leq i \leq 4$, that are eigenvectors of $A_4(u) C_4$ for the eigenvalue λ_i for generic values of u .

These eigenvectors are the starting point of further computations with MATHEMATICA. We give MATHEMATICA many additional substitution rules, taking into account that $u \in [0, 1)$ in the handling of square roots.

The vectors $w_i = A_4(u)^{-1/2}v_i$ are eigenvectors of $A_2(u)^{1/2}C_4A_4(u)^{1/2}$. Since the four eigenvalues are different, the w_i are orthogonal. We take $\tilde{w}_i = n_i^{-1}w_i$ with $n_i = \sqrt{w_i \cdot w_i}$ to get an orthonormal basis. There is the freedom to choose the sign. We multiply \tilde{w}_1 with -1 , to get consistency with our earlier computations.

The \tilde{w}_i can be chosen as the columns of the orthogonal matrix $U(u)$. Then the vectors

$$\tilde{v}_i = A_4(u)^{1/2}\tilde{w}_i = n_i^{-1}v_i(u)$$

are the columns of the transformation matrix $L(u) = A_4(u)^{1/2}U(u)$. In Table 4 we give our choice.

The construction of the v_i allows the components to have singularities. The orthonormalization removes any singularities, so the matrix elements of $L(u)$ are continuous functions on $[0, u_1)$, given by algebraic expressions. An explicit expression for the other transformation matrix $K(u) = A_4(u)^{-1/2}U(u) = A_4(u)^{-1}L(u)$ follows easily.

A check of our computations (including our substitution rules) is carried out, and gives

$$K(u)^T A_4(u) K(u) = I_4, \quad L(u)^T C_4 L(u) = \begin{pmatrix} \frac{9}{14} & 0 & 0 & 0 \\ 0 & \frac{2}{7} & 0 & 0 \\ 0 & 0 & \frac{1}{14} & 0 \\ 0 & 0 & 0 & 0 \end{pmatrix},$$

in accordance with equation (21).

$$\begin{aligned}
L_{1,1} &= \frac{\sqrt{u+6} \left(\sqrt{16-u} (20 - 3(u-4)u) - 18\sqrt{2}\sqrt{5-u}\sqrt{6-u}\sqrt{u} \right)}{192\sqrt{35}(u-5)}, \\
L_{1,2} &= \frac{\sqrt{4-u} \left(\sqrt{2}\sqrt{6-u} (u(3u-22) - 20) + 16\sqrt{5-u}\sqrt{-(u-16)u} \right)}{64\sqrt{105}(u-5)}, \\
L_{1,3} &= \frac{\sqrt{10-u} \left(\sqrt{u} ((28-3u)u - 76) + 2\sqrt{2}\sqrt{5-u}\sqrt{6-u}\sqrt{16-u} \right)}{64\sqrt{21}(u-5)}, \\
L_{1,4} &= -\frac{\sqrt{1200-u(3(u-22)u-484)}\sqrt{40-u(3(u-8)u+64)}}{96\sqrt{14}(u-5)}; \\
L_{2,1} &= \frac{\sqrt{16-u} \left(\sqrt{u+6} (-3(u-16)u - 160) + 18\sqrt{8-2u}\sqrt{5-u}\sqrt{10-u} \right)}{192\sqrt{35}(u-5)}, \\
L_{2,2} &= \frac{\sqrt{6-u} \left(\sqrt{8-2u} (u(3u-38) + 60) + 16\sqrt{5-u}\sqrt{-(u-10)(u+6)} \right)}{64\sqrt{105}(u-5)}, \\
L_{2,3} &= -\frac{\sqrt{u} \left(\sqrt{10-u} (u(3u-32) + 96) + 2\sqrt{8-2u}\sqrt{-(u-5)(u+6)} \right)}{64\sqrt{21}(u-5)}, \\
L_{2,4} &= -\frac{\sqrt{u(-3(u-22)u-484)} + 1200\sqrt{u(-3(u-8)u-64)} + 40}{96\sqrt{14}(u-5)}; \\
L_{3,1} &= \frac{\sqrt{u+6} \left(\sqrt{16-u} (20 - 3(u-4)u) + 18\sqrt{2}\sqrt{5-u}\sqrt{-(u-6)u} \right)}{192\sqrt{35}(u-5)}, \\
L_{3,2} &= \frac{\sqrt{4-u} \left(\sqrt{2}\sqrt{6-u} (u(3u-22) - 20) - 16\sqrt{5-u}\sqrt{-(u-16)u} \right)}{64\sqrt{105}(u-5)}, \\
L_{3,3} &= -\frac{\sqrt{10-u} \left(\sqrt{u} (u(3u-28) + 76) + 2\sqrt{2}\sqrt{5-u}\sqrt{6-u}\sqrt{16-u} \right)}{64\sqrt{21}(u-5)}, \\
L_{3,4} &= -\frac{\sqrt{1200-u(3(u-22)u+484)}\sqrt{40-u(3(u-8)u+64)}}{96\sqrt{14}(u-5)}; \\
L_{4,1} &= -\frac{\sqrt{16-u} \left(\sqrt{u+6} (3(u-16)u + 160) + 18\sqrt{8-2u}\sqrt{5-u}\sqrt{10-u} \right)}{192\sqrt{35}(u-5)}, \\
L_{4,2} &= \frac{\sqrt{6-u} \left(\sqrt{8-2u} (u(3u-38) + 60) - 16\sqrt{5-u}\sqrt{-(u-10)(u+6)} \right)}{64\sqrt{105}(u-5)}, \\
L_{4,3} &= \frac{\sqrt{u} \left(\sqrt{10-u} ((32-3u)u - 96) + 2\sqrt{8-2u}\sqrt{-(u-5)(u+6)} \right)}{64\sqrt{21}(u-5)}, \\
L_{4,4} &= -\frac{\sqrt{1200-u(3(u-22)u+484)}\sqrt{40-u(3(u-8)u+64)}}{96\sqrt{14}(u-5)}.
\end{aligned}$$

Table 4: The transformation matrix $L(u) = A_4(u)^{1/2}U(u)$ that we use to transform the FPU-chain with 4 particles to eigenmodes.

References

- [1] N.Bourbaki, *Éléments de Mathématique, Groupes et algèbres de Lie, Chap. 4, 5 et 6*, Hermann, Paris 1968
- [2] Ognyan Christov, *Non-integrability of first order resonances in Hamiltonian systems in three degrees of freedom*, *Celest. Mech. Dyn. Astr.* 112, pp. 149-167 (2012).
- [3] R.L. Devaney, *Homoclinic orbits in Hamiltonian systems*, *J. Diff. Eqs.* 21, pp. 431-438 (1976).
- [4] J.J. Duistermaat, *Non-integrability of the 1 : 2 : 1 resonance*, *Ergodic Theory and Dynamical Systems* 4, pp. 553-568 (1984).
- [5] E. Fermi, J. Pasta and S. Ulam, *Los Alamos Report LA-1940*, in "E. Fermi, Collected Papers" 2, pp. 977-988 (1955).
- [6] J. Ford, *Physics Reports* 213, pp. 271-310 (1992).
- [7] F.G. Gustavson, *On constructing formal integrals of a Hamiltonian system near an equilibrium point*, *Astron. J.* 71, pp. 670-686 (1966).
- [8] Igor Hoveijn and Ferdinand Verhulst, *Chaos in the 1 : 2 : 3 Hamiltonian normal form*, *Physica D* 44, pp. 397-406 (1990).
- [9] E. Atlee Jackson, *Perspectives of nonlinear dynamics (2 vols.)*, Cambridge University Press (1991).
- [10] Henri Poincaré, *Les Méthodes Nouvelles de la Mécanique Célèste*, 3 vols. Gauthier-Villars, Paris, 1892, 1893, 1899.
- [11] Bob Rink and Ferdinand Verhulst, *Near-integrability of periodic FPU-chains*, *Physica A* 285, pp. 467-482 (2000).
- [12] B. Rink, *Symmetry and resonance in periodic FPU-chains*, *Comm. Math. Phys.* 218, pp. 665-685 (2001).
- [13] J.A. Sanders, F. Verhulst, and J. Murdock, *Averaging methods in nonlinear dynamical systems*, *Applied Mathematical Sciences* vol. 59, 2d ed., Springer, 2007.
- [14] F.E. Udawadia and H. Mylapilli, *Energy control of inhomogeneous nonlinear lattices*, *Roy. Soc. Proc. A* 471:, 20140694 (2015).
- [15] Ferdinand Verhulst, *Methods and applications of singular perturbations*, Springer, 2005.
- [16] Ferdinand Verhulst, *Extension of Poincaré's program for integrability, chaos and bifurcations*, *Chaotic Modeling and Simulation*, October 2011, pp. 3-16.
- [17] Ferdinand Verhulst, *Henri Poincaré, impatient genius*, Springer, 2012.
- [18] Ferdinand Verhulst, *Integrability and non-integrability of Hamiltonian normal forms*, *Acta Applicandae Mathematicae* (2015)
- [19] A. Weinstein, *Normal modes for nonlinear Hamiltonian systems*, *Inv. Math.* 20, pp. 47-57 (1973).